Environmental and Experimental Botany 182 (2021) 104309

Contents lists available at ScienceDirect

Environmental and Experimental Botany

journal homepage: www.elsevier.com/locate/envexpbot

Oxidative stress assessment by a spectroscopic approach in pomegranate plants under a gradient of ozone concentrations

Antonella Calzone [a], Lorenzo Cotrozzi [a,*], Damiano Remorini [a,b], Giacomo Lorenzini [a,b], Cristina Nali [a,b], Elisa Pellegrini [a,b]

[a] Department of Agriculture, Food and Environment, University of Pisa, Via del Borghetto 80, 56124 Pisa, Italy
[b] CIRSEC, Centre for Climate Change Impact, University of Pisa, Via del Borghetto 80, 56124 Pisa, Italy

ARTICLE INFO

Keywords:
Enzymatic and non-enzymatic antioxidants
Gas exchange
O_3
Punica granatum
Spectral signatures
Vegetation index

ABSTRACT

Techniques to monitor oxidative stress pre-visually are essential to optimize plant management. Here, we investigated the capability of hyperspectral reflectance (350–2500 nm) to characterize responses of two pomegranate cultivars (Parfianka and Wonderful) under ozone (O_3) episodes at a gradient of concentrations (50, 100 and 200 ppb for 5 h). Analyzing spectral signatures collected rapidly and non-destructively from asymptomatic leaves, we accurately discriminated the two cultivars, as well as controls from plants exposed to O_3, in particular those under the higher oxidative stress (i.e. 200 ppb). These discriminations were especially accurate in Wonderful at the end of the exposure (5 h from the beginning of exposure; FBE), and at 24 h FBE. Furthermore, using a partial least squares regression (PLSR) approach, we constructed predictive spectral models to estimate from spectra an array of commonly used physiological and biochemical leaf traits related to plant/oxidative stress interaction (photosynthesis, lipid peroxidation, enzymatic and non-enzymatic antioxidants). Most traits were relatively well predicted by spectroscopic models (model goodness-of fit for validation, R^2: 0.77–0.50). Finally, variations of spectra-derived vegetation indices and leaf traits derived from spectra confirmed the lower O_3-tolerance of the Wonderful cultivar, when exposed to 200 ppb. Overall, the present study shows that the proposed spectroscopic approach can rapidly and non-destructively assess early oxidative stress conditions in plants, and consequently it can help in increasing plant yield and quality. Limitations of the approach are also presented and discussed.

1. Introduction

Tropospheric ozone (O_3) is a global air pollutant that causes billions of dollars in lost plant productivity annually, not to mention impairment for ecosystem services (Lefohn et al., 2018). It negatively affects all key features of plant life, from photosynthesis to biomass accumulation. Ozone affects plants both directly, since excessive foliar uptake of O_3 induces oxidative stress to cells if they are not able to repair and/or compensate oxidative damage by the regulation of antioxidant compounds, and indirectly, through its role as a greenhouse gas contributing to global warming (Ainsworth, 2017). Although several efforts have been made to reduce the emission of its precursors (mainly nitrogen oxides and volatile organic compounds), the O_3 concentrations in air are still elevated in many regions of the world (e.g. East Asia), and are predicted to increase further due to both anthropogenic activities (e.g. emission of O_3 precursors) and climatic change (e.g. increased solar radiation and temperature; Lefohn et al., 2018). This raise is especially expected in hot-spot areas such as the Mediterranean basin (Ochoa-Hueso et al., 2017). Therefore, advancements in phenotyping approaches able to early detect and monitor the effects of oxidative stress on plants, even in the absence of visible symptoms, are necessary to increase yield, quality and management promptness and effectiveness (e.g. proper supply of water, fertilizers and agrochemicals), since traditional methods of analyzing such plant responses to variable environments are slow, labor-intensive, and often destructive (Cotrozzi et al., 2018b).

Vegetation spectroscopy is a high-throughput sensor technology based on the optical properties of living vegetation (e.g. leaf and canopy reflectance) that enables the rapid and non-destructive assessment of plant status, along with the potential to simultaneously estimate several plant traits on a large number of individuals over multiple time periods (Cotrozzi and Couture, 2020). The prediction of these traits from leaf

* Corresponding author.
E-mail address: lorenzo.cotrozzi@agr.unipi.it (L. Cotrozzi).

https://doi.org/10.1016/j.envexpbot.2020.104309
Received 27 July 2020; Received in revised form 12 October 2020; Accepted 28 October 2020
Available online 4 November 2020

spectra is based on the exploitation of the relationships of light with molecular organic bonds, mainly C–H, N–H, and O–H, resulting in vibrational excitation at specific wavelengths through the visible (VIS: 400−700 nm), the near-infrared (NIR: 700−1100 nm) and the short-wave infrared (SWIR: 1100−2400 nm) spectral regions (Cotrozzi et al., 2018b). Improvements in the sensitivity and portability of spectrometers, as well as in advancements in computational capacity and chemometric modelling, has enabled the exploitation of reflectance spectra by using different approaches. First, using simple vegetation indices based on the ratio of reflected light at different wavelengths that have been developed to predict several foliar traits (e.g. normalized difference vegetation index, NDVI; Gamon et al., 1995). Second, using multivariate methods (e.g. partial least squares regression, PLSR; Wold et al., 2001) to directly model commonly used foliar morphological, physiological and biochemical plant parameters as a function of the spectral profiles (e.g. Serbin et al., 2015; Couture et al., 2016; Cotrozzi et al., 2017, 2020a, 2020b; Ely et al., 2019; Marchica et al., 2019). Third, using spectra themselves as a phenotypic expression of the aggregate signals of chemical, morphological and physiological properties of leaves under specific environmental conditions (i.e. analyses of spectral signatures; Cotrozzi and Couture, 2020). The ability of vegetation spectroscopy to assess the effects of air pollutants on plants has been reported since long (see Cotrozzi et al., 2018b for a review).

However, questions remain regarding the ability of spectroscopy to detect and monitor the effects of O_3 on vegetation, since (i) most studies were carried out using limited spectral regions; (ii) the available approaches to exploit information from spectra (e.g. spectral indices, multivariate-methods to predict leaf traits, analyses of spectral signatures) were not combined; (iii) chronic O_3 effects have been mostly studied, whereas those of O_3 episodes remain understudied; (iv) a gradient of O_3 concentrations was never investigated; and (v) few species have been studied so far (Marchica et al., 2019). Here, we addressed most of these gaps, focusing on pomegranate, a species never investigated by using a leaf spectroscopy approach (a few spectroscopy studies were performed on pomegranate fruits; e.g. Khodabakhshian et al., 2019).

Pomegranate (*Punica granatum* L.) is a fruit-bearing deciduous shrub in the family Punicaceae, cultivated since ancient times throughout the Mediterranean area and Middle East, and more recently in many other regions world-wide such as in Southern Asia, and North and South America (Texeira da Silva et al., 2013). Although pomegranate is still evaluated as a minor crop, the demand in pomegranate fruits is rapidly increasing because of their large number and content of bioactive and nutraceutic compounds such as vitamins, minerals and polyphenols (Johanningsmeier and Harris, 2011; Singh et al., 2018), as well as the high adaptability of this species to a wide range of environmental constraints such as elevated temperatures, drought and salinity (Texeira da Silva et al., 2013; Catola et al., 2016; Calzone et al., 2020). Only Calzone et al. (2019) investigated the responses of pomegranate (cultivar Dente di cavallo) to realistic and chronic O_3 concentrations (alone and in combination with salinity), whereas the interaction of pomegranate with an episode of O_3 stress was never investigated before the present study.

The aim of the present work was to evaluate the ability of reflectance spectroscopy to rapidly and non-destructively assess the oxidative stress induced by an O_3 episode on asymptomatic pomegranate plants of the two widely cultivated cultivars Parfianka and Wonderful. Specifically, our novel purposes were to (a) evaluate the potential of vegetation spectroscopy to pre-visually and accurately detect oxidative stress conditions induced by a gradient of O_3 concentrations, (b) develop PLSR-models for the estimation from spectra of several commonly investigated leaf traits related to plant-oxidative stress interaction (i.e. photosynthetic activity, lipid peroxidation, antioxidant capacity, and major enzymatic and non-enzymatic antioxidants; Ainsworth, 2017), and (c) investigate the variations of vegetation indices and leaf traits derived from spectra by PLSR-models, under oxidative stress, in order to elucidate the sensitivity of pomegranate cultivars to O_3. Specifically, we predicted that (a) vegetation spectroscopy can early assess oxidative stress, especially when it is of a high magnitude, (b) an array of leaf traits associated with oxidative stress can be accurately predicted from spectra, especially the physiological ones, and (c) variations of predicted leaf traits highlight a higher O_3 tolerance of Parfianka than Wonderful. Most of the outcomes from the present study could be broadly applied across different investigations focused on various abiotic and biotic constraints inducing oxidative stress in plants.

2. Materials and methods

2.1. Plant material and experimental design

On April 2018, two-year-old container-grown pomegranate plants of the commercial cultivars Parfianka and Wonderful were collected from a local nursery and transported to the field-station of San Piero a Grado (Pisa, Italy; 43°40′48″ N, 10°20′46″ E, 2 m a.s.l.) of the Department of Agriculture, Food and Environment, University of Pisa. On August 2018, 45 plants per cultivar were selected for uniformity of height (ca. 1 m), transplanted into 5-L plastic pots containing sandy soil, and maintained well-watered under standard agronomic conditions. After one month (i.e. September 2018), plants were grouped for homogeneity and exposed by four greenhouse fumigation chambers to target O_3 concentrations of 50, 100 and 200 ppb (1 ppb = 1.96 μg m^{-3}, at 25 °C and 101.325 kPa) for 5 h from 10:00 to 15:00, or to charcoal-filtered air (<5 ppb). After the fumigation, all plants were maintained in the same conditions of controls, under charcoal-filtered air. The exposures were performed in three consecutive days: each day, five plants per cultivar were exposed to charcoal-filtered air (i.e. controls) and ten plants per cultivar were exposed to one of the target O_3 concentrations (i.e. 50, 100 and 200 ppb; one O_3 concentration per day; using two chambers for controls and two chambers for plants exposed to O_3; Table S1). Plants were repositioned within each chamber at each time of analysis. The O_3 exposure was performed with a Fisher 500 air-cooled O_3 generator (Fisher America Inc., Houston, TX, USA), according to Cotrozzi et al. (2018a). The greenhouse day and night mean temperatures were 26 and 20 °C, respectively; and maximum day and night of relative humidity (RH) were approximately 60 and 50 %, respectively.

Measurements and sampling were carried out at 0, 1, 2, 5, 7 and 24 h from the beginning of exposure (FBE). This timing was in accordance with previous studies focused on stress episodes in herbaceous and tree species (e.g. Pellegrini et al., 2018; Landi et al., 2019; Pistelli et al., 2019). At each time of analysis of each of the three days of the experiment, leaf reflectance profiles of five controls and ten O_3-treated plants of each cultivar (two leaves per plant) were collected in a few minutes. These reflectance measurements (n = 540) were used for the analyses of spectral signatures and for the final estimations of vegetation indexes and other leaf traits predicted by PLSR-models here developed (see below). After these spectral measurements, one control plant and two ozonated plants of each cultivar were selected at each time FBE (except at 0 FBE) and consecutively measured/harvested in the following order: leaf gas exchanges, reflectance and sampling. This procedure was so performed once on each plant (n = 90) throughout the whole experiment. Gas exchange measurements were performed on the third highest, mature and fully-expanded leaf, whereas similar and contemporary leaves (three per plant) were collected in liquid nitrogen, stored at −80 °C, and later freeze-dried for biochemical analyses. These combined spectral and standard measurements (i.e. gas exchange and biochemistry) were used to build PLSR-models (see below). The onset of visible foliar symptoms was checked throughout the whole experiment.

2.2. Collection of leaf spectra

Full range (350−2500 nm) leaf reflectance profiles were collected using an ASD FieldSpec 4 spectroradiometer (Analytical Spectral

Devices, Boulder, CO, USA), equipped with a leaf-clip including an internal halogen light source attached to a plant probe. Measurements were collected on two areas (randomly selected, Ø 1 cm) of the adaxial surface of each leaf, with one measurement per area, and collections were combined to produce an average leaf spectrum. The relative reflectance of each leaf was determined from the measurement of leaf radiance divided by the radiance of a white reference panel included in the leaf-clip, measured every 12 spectral collections.

2.3. Standard measurements

Carbon dioxide (CO_2) assimilation rate (A), transpiration (E), stomatal conductance (g_s) and intercellular CO_2 concentration (C_i) were determined using an infra-red gas-analyzer (CIRAS-2, PP Systems International Inc., Amesbury, MA, USA) equipped with a leaf chamber set to 400 ppm of CO_2 concentration, 1500 µmol m^{-2} s^{-1} of PAR (i.e. saturating light conditions), and 65 % of RH. Average leaf temperature and vapor pressure deficit inside the cuvette were 28 °C and 2.0 kPa, respectively. Intrinsic water use efficiency (WUE_{in}) was determined as A/g_s.

A UV-1900 spectrophotometer (Shimadzu, Kyoto, Japan) was used for all spectrophotometric analyses, unless otherwise specified. After extracting 10 mg of leaf samples with 1 mL of 80 % ethanol, lipid peroxidation was determined by measuring the malondialdehyde (MDA) by-product accumulation (Hodges et al., 1999), which takes into account the possible influence of interfering compounds in the assay (e.g., phenols) for the 2-thiobarbituric acid-reactive substances (Guidi et al., 2016). The antioxidant ability was evaluated by measuring the oxygen radical absorption capacity (ORAC; Ou et al., 2001) and hydroxyl radical antioxidant capacity (HORAC; Ou et al., 2002), on 10 mg of leaf samples extracted with 1 mL of methanol, and using fluorescein as fluorescent probe. The antioxidant scavenging activity was induced by a free radical initiator, 2,2′-azobis-(2-amidino-propane) dihydrochloride and Co(II) complex, and quantified with excitation at 480 nm and emission at 530 nm, using a Victor3 1420 Multilabel Counter (Perkin Elmer Inc., Waltham, MA, USA). Fluorescence/absorbance quantified with antioxidant standard curves were expressed in Trolox and gallic acid equivalents for ORAC and HORAC, respectively.

Superoxide dismutase (EC 1.15.1.1) activity (SOD_{act}) was defined on leaf extracts [50 mg in 1 mL of K-phosphate buffer (50 mM, pH 7), containing glycerol 10 % (v/v), polyvinylpyrrolidone 1% (w/v), Triton X-100 0.1 % (v/v) and 1 mM EDTA] as the amount of superoxide dismutase required to cause 50 % inhibition of the rate of nitroblue tetrazolium reduction, assessed by its absorbance at 560 nm (Zhang and Kirkham, 1994); whereas catalase (EC 1.11.1.6) activity (CAT_{act}) was evaluated on leaf extracts (100 mg in 0.6 mL of the same buffer used for SOD_{act} determination) as the decomposition of hydrogen peroxide (H_2O_2) within one minute, assessed as the decrease in absorbance at 240 nm (Aebi, 1984). After extraction of 40 mg of leaf samples with 0.4 mL of Na-phosphate buffer (50 mM, pH 7.0) containing 1 mM EDTA, 0.1 % (v/v) Triton X-100, 10 % (v/v) glycerol and 5 mM ascorbate, ascorbate peroxidase (EC 1.11.1.11) activity (APX_{act}) was determined with the method of Mittler and Zilinskas (1993), by measuring the oxidation of ascorbate at 290 nm for 1 min (at 25 °C). For enzymatic assays, protein concentrations were determined according to Bradford (1976).

Total ascorbate (Asc) content was determined extracting 10 mg of leaf samples with 1 mL of 6 % trichloroacetic acid (TCA, w/v), and then running an assay based on the reduction of ferric ion (Fe^{3+}) to ferrous ion (Fe^{2+}) with ascorbate in acid solution, followed by the formation of the red chelate between Fe^{2+} and 2,2′-dipyridyl (Kampfenkel et al., 1995). Absorbances were recorded at 525 nm and quantified with an Asc standard curve. Total glutathione (Glut) content was determined extracting 10 mg of leaf samples with 1 mL of 5% TCA, and then following an enzymatic recycling procedure in which glutathione is sequentially oxidized by 5,5′-dithiobis-2-nitrobenzoic acid and reduced by NADPH in the presence of glutathione reductase (Sgherri and Navari-Izzo, 1995). Absorbances were recorded at 412 nm and quantified with a Glut standard curve.

Total phenols (Phen) were extracted from 5 mg of leaf samples with 1.9 mL of 95 % methanol for 48 h in the dark, and determined by the Folin-Ciocalteu method, according to Ainsworth and Gillespie (2007). Absorbances were recorded at 765 nm and quantified as gallic acid equivalents, using a standard curve. Total anthocyanins (Ant) were extracted from 20 mg of leaf samples with 0.5 mL of 95 % acidified ethanol (0.225 N HCl), according to Cevallos-Casals and Cisneros-Zevallos (2003) with minor modifications. Spectrophotometric readings at 510 nm were taken subtracting absorbance at 700 nm (due to turbidity). Total anthocyanins were expressed as cyanidin 3-glucoside equivalents, using a molar extinction coefficient of 25,965 M^{-1} cm^{-1} and a molecular weight of 449 g mol^{-1}.

2.4. Analyses of spectral signatures

The effects of cultivar, O_3, time and their interactions on the untransformed reflectance profiles of pomegranate (averaged per plant, only data interpolations and profile jump corrections were performed) were assessed by permutational multivariate analysis of variance (PERMANOVA; Anderson, 2001), employing Euclidian measurements of dissimilarity and 10,000 permutations. Permutational multivariate analysis of variance was also used to test the effects of cultivar, O_3 and their interaction, keeping times of meassurement separated; and the influence of O_3, time and their interaction, keeping cultivars separated. Finally, PERMANOVA was also used to determine the influence of O_3 on reflectance profiles at each time of analysis, keeping both cultivars and times of analysis separated; and principal coordinates analysis (PCoA) was used on these spectral data to visualize the spectral responses at all times of analysis (i.e. 0, 1, 2, 5, 7 and 24 h FBE), always using Euclidean distances through the 'vegan' package in R (www.r-project.org; Dixon, 2003). Principal coordinates analysis utilizes a distance of uncorrelated variables, or principal coordinates, reducing the dimensionality of the data.

The capability of spectroscopy to classify experimental groups, for which significant effects were observed by PERMANOVA was further determined by partial least squares-discriminant analysis (PLS-DA; Chevallier et al., 2006). According to PERMANOVA approach, PLS-DA was firstly used on all spectral profiles and then on subsets related to separated times of analysis. Partial least squares-discriminant analysis is a statistical analysis utilized with high dimensional data to discriminate groups by projecting latent variables through the response and predictor variables to both reduce data dimensionality and maximize prediction accuracy. The PLS model fits response variables that are indicators of groups of interest to the spectrum. This is an appropriate method for data in which predictor variables have a high degree of collinearity (Cotrozzi and Couture, 2020). The analyses were run 500 times by dividing observations into different groups of calibration (training) and validation (testing) sets, and the number of correct classifications both in the calibration and in the validation sets across the 500 iterations was used to determine the accuracy of the tested model. The calibration:validation data ratio and the number of components used to get the models that would give the best fit to the data were determined by iteratively running the PLS-DA models with different calibration:validation data ratio (i.e. 50:50, 70:30, 80:20) and numbers of components, and were based on the highest *kappa* values returned for the validation models. Partial least squares-discriminant analysis was run with the 'caret' and 'vegan' packages in R (www.r-project.org; Dixon, 2003; Kuhn, 2008).

2.5. PLSR-model calibration and validations

Fifteen leaf traits (i.e. A, g_s, C_i, E, WUE_{in}, MDA, ORAC, HORAC, SOD_{act}, CAT_{act}, APX_{act}, Asc, Glut, Phen and Ant) were predicted from spectra using a PLSR (Wold et al., 2001) modeling approach, using untransformed reflectance profiles (only data interpolations and profile jump corrections were performed). This 'spectra-trait' modeling was

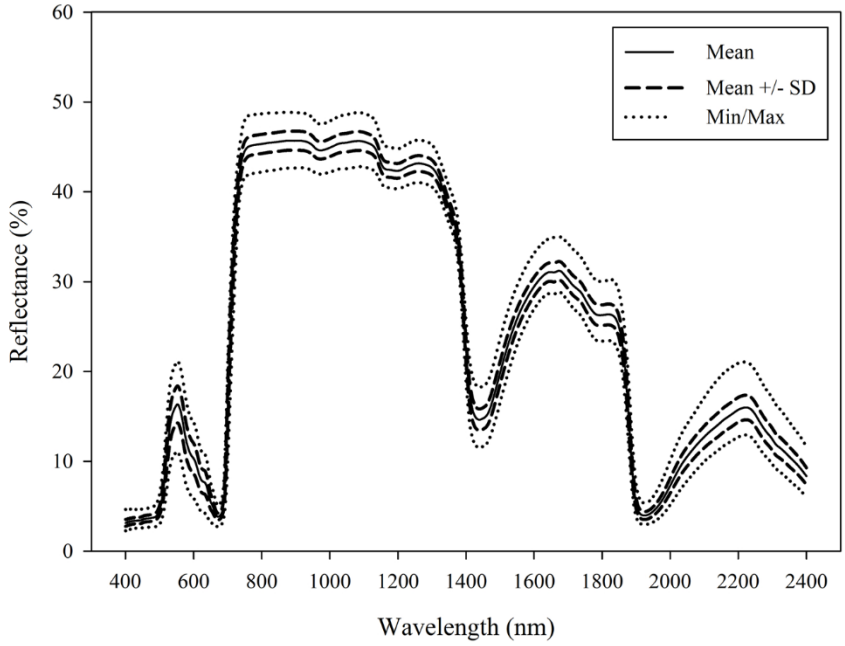

Fig. 1. Summary of leaf spectral measurements repeatedly collected (0, 1, 2, 5, 7 and 24 h from the beginning of exposure) on pomegranate cultivars (Parfianka and Wonderful) exposed to a gradient of ozone concentrations (0, 50, 100 and 200 ppb), and devoted to the analyses of spectral signatures. The mean, mean ± standard deviation (SD), minimum and maximum leaf reflectance for all samples (n = 540) are shown.

Table 1
F and *P* values of three-way permutational analysis of variance (PERMANOVA) for the effects of cultivar, ozone (O_3), time and their interactions on full range (400-2400 nm) reflectance profiles of pomegranate leaves. *df* represents the degrees of freedom. ***: $P \leq 0.001$, **: $P \leq 0.01$, ns: $P > 0.05$. *P* value of the Cultivar × O_3 interaction is *ns* (italicized) because equal to 0.061 (marginally significant).

Effect	*df*	F	*P*
Cultivar	1	22.35	***
O_3	3	13.44	***
Time	5	2.59	**
Cultivar × O_3	3	1.90	*ns*
Cultivar × Time	5	0.79	ns
O_3 × Time	15	0.83	ns
Cultivar × O_3 × Time	15	0.73	ns

conducted using ca. 80 % of the whole dataset, in order to allow also an external validation of the developed PLSR-models (see below). In contrast to classical regression techniques, PLSR reduces a large number of collinear predictor variables (as in the case with hyperspectral data) into relatively few, uncorrelated latent variables, avoiding the risk of producing unreliable coefficients and error estimates (Grossman et al., 1996), thus becoming the favorite method for chemometric approaches (e.g. Atzberger et al., 2010; Couture et al., 2016; Cotrozzi et al., 2017; Ely et al., 2019). To avoid potential overfitting the models, the numbers of latent variables to use were identified based on reduction of the predicted residual sum of squares (PRESS) statistics (Chen et al., 2004) using leave-one-out cross-validation. Finally, the selected sets of extracted components were combined into linear models predicting leaf traits from leaf reflectance profiles.

Model performance was assessed by running 500 randomized permutations of the datasets using 80 % of the data for calibration and the remaining 20 % for validation (i.e. internal validation). To assess model performance, we calculated the model goodness-fit (R^2), the overall error rate (RMSE, root-mean-square error), the bias and the percentage of error over the data range (%RMSE), when applied to the calibration and the validation datasets. These randomized analyses produced a distribution of fit statistics allowing for the evaluation of model stability as well as uncertainty in model predictions. The strength contribution of PLSR loadings by individual wavelengths was also assessed using the variable important to the projection (VIP) selection statistics, which highlight the importance of individual wavelengths in explaining the variation in both the response and predictor variables: larger weightings confer higher value to contribution of individual wavelengths to the predictive model (Wold et al., 2001; Chong and Jun, 2005). The modelling approach and data analyses were performed using the 'pls' package in R (www.r-project.org; Mevik et al., 2016).

Before developing the final modelling, we tested preliminary models to identify poorly predicted outliers. Prediction residuals were investigated to identify potential outliers (Couture et al., 2016). Spectral profiles of outliers were further examined for errors (e.g. elevated reflectance in the VIS wavelengths, spectral jumps produced by misaligned detector splicing, concave spectral shape at the red-edge peak) all likely due to operational errors during spectral collections (in reference or target measurements). Standard measurements of outliers were also investigated for extremes in the data distribution. Outliers removed accounted for approximately 15 % of the initial data, according to previous studies (e.g. Couture et al., 2016; Marchica et al., 2019)

We additionally performed an external validation by applying PLSR-coefficients on a dataset distinct from the one used for calibration and validation (ca. 20 % of the whole dataset). Relations between predicted and observed values were tested by regression analysis, and fit statistics (i.e. R^2, RMSE, bias) were again used to assess model estimation accuracy.

2.6. Estimation of leaf traits by vegetation indices and PLSR-models

Four common vegetation indices were calculated from spectra: the normalized difference vegetation index [NDVI=(R_{780}-R_{570})/(R_{780}+R_{570}); Gamon et al., 1995] was determined to evaluate the potential occurrence of (sub)visible symptoms; the photochemical reflectance index [PRI=(R_{531}-R_{570})/(R_{531}+R_{570}); Gamon et al., 1997; scaled as sPRI=(PRI+1)/2 to avoid negative values] was determined to assess any potential effect on photochemical system; the plant senescence reflectance index [PSRI=(R_{678}-R_{500})/R_{750}; Merzlyak et al., 1999; scaled as sPSRI=(PSRI+1)/2 to avoid negative values] was determined to evaluate

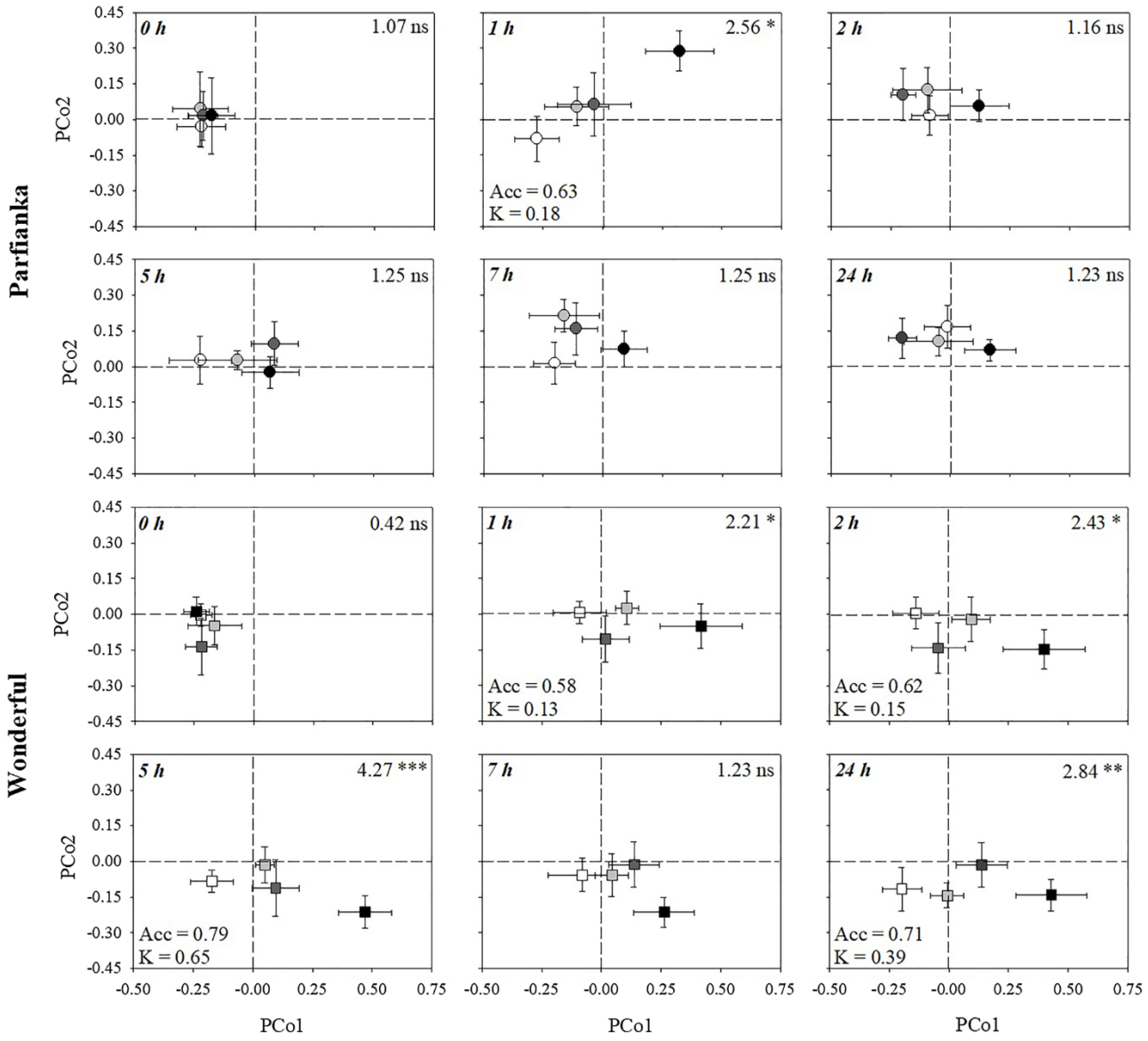

Fig. 2. Scores (mean ± standard error) for the first and second principal components from principal coordinates analysis (PCoA) of reflectance data (400-2400 nm) collected from leaves of pomegranate cultivars Parfianka (circle) and Wonderful (square), highlighting the ability of hyperspectral data to detect the effects of a gradient of ozone (O_3) concentrations (0 ppb, white; 50 ppb, light gray; 100 ppb, dark gray; 200 ppb, black; for 5 h) at 0, 1, 2, 5, 7 and 24 h from the beginning of exposure. For each cultivar and time, F and *P* values from permutational analysis of variance (PERMANOVA) for the effects of O_3 on full range (400-2400 nm) reflectance profiles of pomegranate leaves are shown on the top right corner of panels (***: $P \leq 0.001$, **: $P \leq 0.01$, *: $P \leq 0.05$, ns: $P > 0.05$). In cases where PERMANOVA reveals a significant O_3 effect, accuracy (Acc) and *kappa* (K) values from partial least squares discriminant analysis (PLS-DA) are also shown on the bottom left corner of panels.

the occurrence of any potential senescence process; and a carotenoid reflectance index [CRI=$(R_{510})^{-1}$-$(R_{550})^{-1}$; Gitelson et al., 2002] was determined to investigate any potential accumulation of carotenoids as defense response. R_x indicates reflectance at x nm wavelength.

Other leaf traits were estimated from spectra by using the best performing PLSR-models. As already stated above, vegetation indices and spectra-derived leaf traits were calculated from spectra averaged per plant.

2.7. Statistical analysis of leaf traits derived from spectra

Collected samples were analyzed all together, using the plant as experimental unit. The Shapiro-Wilk test was firstly used to assess the normal distribution of spectral indices and leaf traits derived from spectra by PLSR-models. The effects of cultivar, O_3, time and their interactions on these leaf traits were then investigated by a three-way repeated measures analysis of variance (ANOVA). Tukey's test was used as *post-hoc* test. Statistically significant effects were considered for $P \leq 0.05$. Univariate statistical analyses were run in JMP 13.2.0 (SAS Institute Inc., Cary, NC, USA).

3. Results

3.1. Leaf spectral signatures

Keeping in mind that no visible symptoms were observed during all three days of analysis (some O_3-induced minute brownish necrosis was observed only after 5 days FBE on the adaxial surface of 3–4 leaves per cultivar exposed to 200 ppb), a summary of leaf reflectance measurements devoted to the analyses of spectral signatures is reported in Fig. 1. The largest ranges in reflectance generally coincided with typical features of foliar reflectance such as the peak at around 550 nm in the VIS,

Table 2
Range, number of components (comp), model goodness-fit (R^2), root-mean square error (RMSE) and bias for calibration (Cal) and validation (Val) data generated using 500 random permutations of the data with 80 % used for cal and 20 % used for val for PLSR-models predicting leaf traits from pomegranate spectra. Data are shown as mean ± standard deviation. Bias for Cal is not shown since it was always <0.001. Trait abbreviations: A, CO_2 assimilation rate (μmol m^{-2} s^{-1}); E, transpiration (mmol m^{-2} s^{-1}); g_s, stomatal conductance (mol m^{-2} s^{-1}); C_i, intercellular CO_2 concentration (μmol mol^{-1}); WUE_{in}, intrinsic water use efficiency (μmol mol^{-1}); MDA, malondialdehyde (μmol g^{-1} DW); ORAC, oxygen radical absorption capacity (mmol TE g^{-1} DW); HORAC, hydroxyl radical antioxidant capacity (mmol GAE g^{-1} DW); SOD_{act}, superoxide dismutase activity (U mg^{-1} protein); CAT_{act}, catalase activity (U mg^{-1} protein); APX_{act}, ascorbate peroxidase activity (U mg^{-1} protein); Asc, total ascorbate (μmol g^{-1} DW); Glut, total glutathione (μmol g^{-1} DW); Phen, total phenols (mmol GAE g^{-1} DW); Ant, total anthocyanins (μmol C3GE g^{-1} DW). DW: dry weight; TE: trolox equivalents; GAE: gallic acid equivalents; C3GE: cyanidin 3-glucoside equivalents.

Trait	Range	Comp	Cal		Val		
	(nm)		R^2	RMSE	R^2	RMSE	Bias
A	400–900	10	0.73 ± 0.07	0.76 ± 0.05	0.37 ± 0.29	1.20 ± 0.26	−0.05 ± 0.38
E	400–900	13	0.91 ± 0.02	0.11 ± 0.01	0.60 ± 0.17	0.24 ± 0.05	0.00 ± 0.08
g_s	400–900	10	0.80 ± 0.03	0.04 ± 0.00	0.48 ± 0.22	0.06 ± 0.01	0.00 ± 0.02
C_i	400–900	14	0.96 ± 0.02	3.04 ± 0.31	0.60 ± 0.28	7.96 ± 2.17	−0.57 ± 2.90
WUE_{in}	400–900	10	0.78 ± 0.04	0.87 ± 0.06	0.50 ± 0.22	1.35 ± 0.23	−0.01 ± 0.39
MDA	600–900	12	0.89 ± 0.02	4.52 ± 0.50	0.56 ± 0.18	9.03 ± 1.74	0.29 ± 3.01
ORAC	400–800	17	0.97 ± 0.01	0.10 ± 0.01	0.61 ± 0.20	0.52 ± 0.11	0.00 ± 0.16
HORAC	950–2400	11	0.86 ± 0.03	0.17 ± 0.02	0.44 ± 0.23	0.36 ± 0.08	0.01 ± 0.12
SOD_{act}	600–900	14	0.97 ± 0.01	4.85 ± 0.67	0.50 ± 0.22	21.36 ± 5.11	0.20 ± 6.68
CAT_{act}	1400–2400	9	0.56 ± 0.06	2.26 ± 0.17	0.14 ± 0.19	3.52 ± 0.65	−0.02 ± 1.15
APX_{act}	400–2400	15	0.93 ± 0.02	−3e-21 ± 5e-20	0.44 ± 0.27	1e-8 ± 3e-6	0.00 ± 0.00
Asc	1100–1800	8	0.71 ± 0.03	0.94 ± 0.06	0.45 ± 0.22	1.33 ± 0.24	−0.02 ± 0.45
Glut	500–1100	9	0.84 ± 0.04	3.91 ± 0.50	0.37 ± 0.25	9.73 ± 2.65	−0.43 ± 3.90
Phen	1600–2400	11	0.93 ± 0.01	0.05 ± 0.00	0.77 ± 0.12	0.09 ± 0.02	0.00 ± 0.03
Ant	1400–1800	13	0.97 ± 0.01	0.03 ± 0.01	0.59 ± 0.19	0.32 ± 0.06	−0.01 ± 0.11

throughout the NIR (800–1300 nm) characterized by high reflectivity, and peaks in the SWIR region centered at 1700, 1800 and 2200 nm.

After testing several spectral ranges to get highest significances from PERMANOVA that was run to test the effects of cultivar, O_3, time and their interactions on leaf reflectance profiles (Table S2), the best results were recorded using the full range (i.e. 400–2400 nm). Final PERMANOVA showed that cultivar, O_3 and time affected the reflectance profile of pomegranate leaves (Table 1). According to PLSDA, the best classifications of cultivars, O_3 concentrations and times of analysis from spectra (higher *kappa*) occurred with a 80:20 ratio for calibration:validation data using 20, 45 and 50 components, respectively: classification accuracy and *kappa* were 0.96 ± 0.02 and 0.92 ± 0.04, 0.65 ± 0.05 and 0.53 ± 0.06, and 0.84 ± 0.04 and 0.81 ± 0.04, respectively (data are shown as mean ± standard deviation). Only a marginally significant effect ($P = 0.06$) was observed for the interaction cultivar × O_3, whereas no significant effects were found for the other bi- and tri-factorial interactions (Table 1). The bi-factorial effects cultivar × O_3 and O_3 × time were also not significant keeping times of analysis or cultivars separated, respectively (Tables S3 and S4). However, keeping both cultivars and times of analysis separated, PERMANOVA showed significant O_3 effects on Parfianka profiles at 1 h FBE, and on Wonderful ones at 1, 2, 5, and 24 h FBE (Fig. 2, showing PCoA results). According to PLS-DA (80:20 ratio for calibration:validation data), good classifications among O_3 concentrations occurred in Wonderful at 5 and 24 h FBE (components, accuracy and *kappa*: 20, 0.79 ± 0.05 and 0.65 ± 0.04, and 20, 0.71 ± 0.02 and 0.39 ± 0.04, respectively), whereas lower classification accuracies were found in Parfianka at 1 h FBE (components, accuracy and *kappa*: 18, 0.63 ± 0.03, 0.18 ± 0.02), as well as in Wonderful at 1 and 2 h FBE (components, accuracy and *kappa*: 18, 0.58 ± 0.02 and 0.13 ± 0.04, and 24, 0.62 ± 0.02 and 0.15 ± 0.04, respectively). Highest O_3 concentration (i.e. 200 ppb) was well discriminated, while 50 and 100 ppb levels were mostly misclassified, and were sufficiently discriminated from 0 ppb condition only in Wonderful at 5 and 24 h FBE.

3.2. PLSR prediction models

We preliminary tested numerous PLSR-models containing several wavelength ranges, including characteristic absorption features (Curran, 1989) to optimize the statistical results (i.e. to obtain highest model R^2 and lowest RMSE and bias) for the predictions of A, E, g_s, C_i, WUE_{in}, MDA, ORAC, HORAC, SOD_{act}, CAT_{act}, APX_{act}, Asc, Glut, Phen and Ant from leaf spectra (Table S2). Final models for gas-exchange traits (A, E, g_s, C_i and WUE_{in}) utilized the wavelengths from 400–900 nm, using 10, 13, 10, 14 and 10 components, respectively (Table 2). Similar spectral ranges were used in final models for MDA (600–900 nm, 12 components), ORAC (400–800 nm, 17 components), SOD_{act} (600–900, 14 components) and Glut (500–1100 nm, 9 components). Final models of the other leaf traits utilized longer NIR-SWIR regions: 950–2400 nm for HORAC (11 components), 1400–2400 nm for CAT_{act} (9 components), 1100–1800 nm for Asc (8 components), 1600–2400 nm for Phen (11 components), and 1400–1800 nm for Ant (13 components). Only the final model for APX_{act} was built using the full range (i.e. 400–2400 nm), including 15 components. Table 2 summarizes these outcomes for PLSR-models, as well as the statistical outputs related to their performance.

Model performance was high for Phen, ORAC, E, C_i and Ant (R^2 and %RMSE for validation: 0.77 and 16 %, 0.61 and 11 %, 0.60 and 18 %, 0.60 and 8%, 0.59 and 15 %, respectively), and moderate for MDA, WUE_{in} and SOD_{act} (R^2 and %RMSE for validation: 0.56 and 17 %, 0.50 and 13 %, 0.50 and 16 %, respectively), while lower prediction performance was found for g_s, HORAC, APX_{act} and Asc (R^2 and %RMSE for validation: 0.48 and 18 %, 0.44 and 16 %, 0.44 and 15 %, 0.45 and 16 %). Insufficient model performance was instead reported for A, Glut and CAT_{act}. Statistical outputs for PLSR-model performances are reported in Table 2 and Fig. 3. PLSR-model fit statistics for external validations were similar to those registered for validations, except for HORAC that were slightly lower (Table S5).

Standardized coefficients and VIP metrics (Fig. S1) showed wavelengths from 650 to 750 nm as most important for predictions of gas-exchange traits (A, E, g_s, C_i and WUE_{in}; Fig. 3B,D,F,H,J), as well as of MDA, ORAC, SOD_{act}, and Glut; whereas around 1400, 1700 and 1900 nm for HORAC and CAT_{act}, around 1700 and 1900 nm also for Phen, and around 1650 nm for Ant. Finally, the whole VIS and wavelengths around 750 nm, together with spectral regions around 1400 and 1900 nm resulted most important for APX_{act} prediction.

3.3. Vegetation indices and leaf traits predicted from spectra

Table 3 shows the effects of cultivar, O_3, time and their interactions on vegetation indices and selected leaf traits predicted from spectra. We investigated only the leaf traits predicted by PLSR models with a validation R^2 greater than or equal to 0.5. Normalized different vegetation

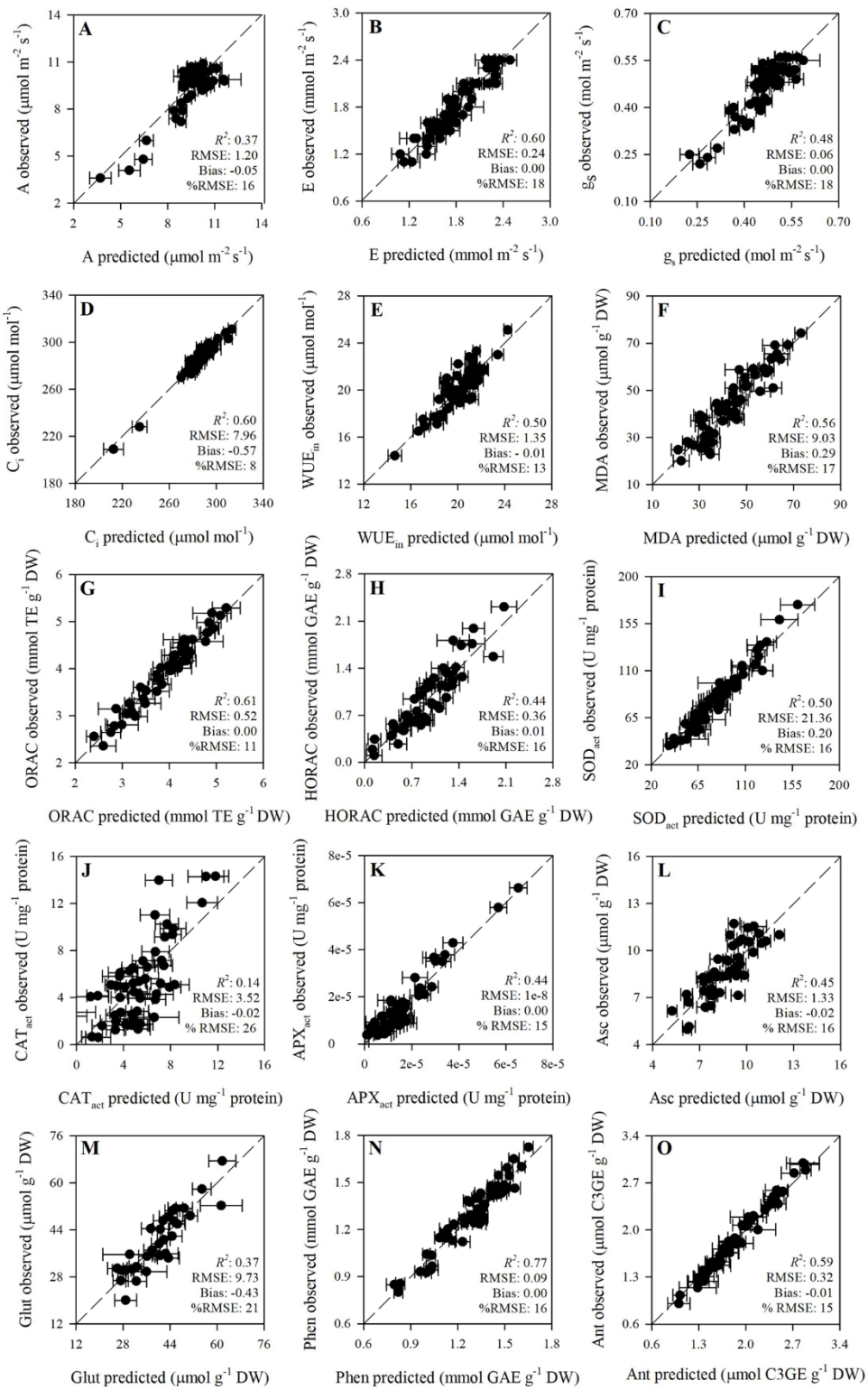

Fig. 3. Observed vs partial least squares regression (PLSR)-predicted values of leaf traits related to plant-oxidative stress interaction in pomegranate; error bars for predicted values represent the standard deviations generated from 500 simulated models; dashed line is 1:1 relationship; model goodness-fit (R^2), root-mean-square error (RMSE), bias and %RMSE for validation data generated using 80 % of the data for calibration and 20 % for validation are reported. See Table 2 caption for trait abbreviations.

index and sPSRI only showed a significant O_3 effect, slightly decreasing only under 200 ppb (-6 and -2 % in comparison with controls, respectively, averaging cultivars and times of analysis; *data not shown*). A similar O_3 effect was also observed on E, which significantly decreased of 7 % under 200 ppb (means: 1.68 vs 1.80 mmol m^{-2} s^{-1}; E also showed significant time and cultivar × time effects, actually). Intercellular CO_2 concentration was not affected by O_3, showing only a significant time effect. Conversely, a significant cultivar × O_3 interaction was found for sPRI and SOD_{act} (with SOD_{act} also showing a significant O_3 × time interaction), and a significant cultivar × O_3 × time interaction was observed for CRI, WUE_{in}, MDA, ORAC, Phen and Ant. Variations of these leaf traits are reported in Figs. 4–7. Scaled photochemical reflectance index slightly decreased only in Parfianka under 200 ppb (−1 %, Fig. 4B), while SOD_{act} decreased in both cultivars under 200 ppb, but more in Parfianka than in Wonderful (−24 vs −19 %, respectively; Fig. 6A). Intrinsic water use efficiency decreased in both cultivars under

Table 3
F and *P* values of three-way repeated measures analysis of variance (ANOVA) for the effects of cultivar, ozone (O_3), time and their interactions on spectral indices and leaf traits derived from pomegranate spectra. Only leaf traits derived by PLSR models with a validation R^2 greater than or equal to 0.5 were selected. *df* represents the degrees of freedom. ***: $P \leq 0.001$, **: $P \leq 0.01$, *: $P \leq 0.05$, ns: $P > 0.05$. Trait abbreviations: NDVI, normalized different vegetation index; sPRI, photochemical reflectance index (scaled); CRI, carotenoid reflectance index; sPSRI, plant senescence reflectance index (scaled); E, transpiration; C_i, intercellular CO_2 concentration; WUE_{in}, intrinsic water use efficiency; MDA, malondialdehyde; ORAC, oxygen radical absorption capacity; SOD_{act}, superoxide dismutase activity; Phen, total phenols; Ant, total anthocyanins.

Effect	*df*	NDVI	sPRI	CRI	sPSRI	E	C_i	WUE_{in}	MDA	ORAC	SOD_{act}	Phen	Ant
Cultivar	1	2.65ns	63.88***	8.51**	0.63ns	0.30ns	0.00ns	0.50ns	132.51***	10.75**	2.67ns	0.02*	139.19***
O_3	3	8.27***	3.35*	2.70*	3.05*	10.88***	0.59ns	54.39***	13.52***	6.17***	19.94***	24.28***	10.00***
Time	3	0.35ns	10.99***	0.30ns	2.60ns	19.60***	4.63***	29.91***	5.26***	8.35***	3.44*	3.09**	3.23**
Cultivar × O_3	5	2.06ns	4.15**	17.81***	2.61ns	1.82ns	1.78ns	8.67***	12.29***	8.75***	15.62***	29.79***	4.43**
Cultivar × *Time*	5	0.47ns	1.55ns	4.63***	0.81ns	2.42*	1.68ns	8.03***	1.53ns	6.52***	0.98ns	2.01ns	1.05ns
O_3 × *Time*	15	0.68ns	0.55ns	3.46***	0.58ns	1.28ns	0.66ns	16.86***	1.84*	5.90***	2.36**	1.92*	1.12ns
Cultivar × O_3 × *Time*	15	0.48ns	0.96ns	3.03***	0.45ns	0.91ns	0.50ns	6.36***	1.78*	1.83*	0.66ns	1.79*	2.13**

200 ppb at 5 h FBE (-23 %), but only in Wonderful decreased again at 24 h FBE (-28 %), after a recovery at 7 h FBE (Fig. 4A). Malondialdehyde increased only in Wonderful under 100 ppb at 5 h FBE (+50 %), and under 200 ppb from 2 to 24 h FBE (+69 %, as average; Fig. 5A). Oxygen radical absorption capacity values were lower in Parfianka exposed to 50 ppb than in respective controls at 5 h FBE (-57 %), whereas increased in Wonderful under 200 ppb at 2 h FBE (+70 %, Fig. 5B). Carotenoid reflectance index was only affected by 100 ppb, decreasing in Parfianka at 5 h FBE (-38 %), whereas increasing in Wonderful at 2 and 7 h FBE (+39 and +51 %, respectively; Fig. 6B). Phenols only decreased in Wonderful under 100 ppb at 5 h FBE (-24 %), and under 200 ppb from 1 to 24 h FBE (-30 %, as average; Fig. 7A). Anthocyanins only decreased in Wonderful under 200 ppb at 5 h FBE (-58 %, Fig. 7B).

4. Discussion

The first major achievement of the present study was the evidence that we were able to distinguish with high accuracy the pomegranate cultivars (almost visually identical during the whole vegetative phase) using the full range spectral region (i.e. 400−2400 nm), as well as the sensitivity of the reflectance profiles to O_3 exposure and time. Specifically, even in the absence of visible symptoms (they occurred only five days FBE on very few leaves exposed to 200 ppb of O_3), we were able to discriminate controls from plants exposed to increasing O_3especially those under the highest O_3 level (i.e. 200 ppb), while misclassification occurred between samples exposed to 50 and 100 ppb. However, the bi- and tri-factorial interactive effects on spectral profiles were not detected, except for the marginally significant ($P = 0.06$) cultivar × O_3 interaction (cultivar × O_3 and O_3 × time effects were not detectable also keeping times of analysis or cultivars separated, respectively). This might be due to an O_3 tolerance of pomegranate, but better outputs might be reached by raising the experimental/plant replications. This limitation in prediction accuracy of interactive effects by spectroscopic data has been already reported (Cotrozzi and Couture, 2020). However, keeping cultivars and times of measurement separated, we were able to distinguish an O_3 effect already at 1 h FBE (when none of the traits reported below showed a significant effect) in both cultivars, as well as at 2, 5 and 24 h FBE only in Wonderful. These discriminations resulted highly accurate especially in Wonderful at 5 and 24 h FBE. Again, the effect of the highest O_3 concentration was more evident on spectral profiles. The effects of 50 and 100 ppb O_3 levels were misclassified, and were indeed distinguishable from controls only in Wonderful at 5 and 24 h FBE. On the one hand, these results confirm the capability of this approach (i.e. analyses of spectral signatures) to detect early oxidative stress induced by O_3, as previously reported for various abiotic and biotic stressors (e.g. Marchica et al., 2019; Campos-Medina et al., 2019; Begum et al., 2020; Cotrozzi and Couture, 2020; Gongora-Canul et al., 2020); on the other hand, they show that the efficiency of this spectral approach is dependent on the sensitivity of plants/cultivars to oxidative stress, as well as to the magnitude at which this environmental stress is imposed on vegetation: the approach works better when the impact of oxidative stress on plants (and thus on their spectral profiles) is higher.

We thus encourage the use and development of this spectroscopy approach (i.e. utilization of full range spectral data as a phenotypic expression of leaves under specific environmental conditions; Cavender-Bares et al., 2016), since spectral signatures of plants could potentially provide important information for plant selection and management, more than focusing on individual traits that are often not sufficient to monitor and manage plant productivity and quality. However, high-throughput measurements of specific leaf traits is also necessary since the prediction of these outcomes, in combination with analyses of spectral signatures, has the potential to provide multiple layers of stress-specific information to growers, including the identification of the underlying leaf responses, that can further increase the efficiency of management practices (Cotrozzi and Couture, 2020).

Effectively, the second major and novel achievement of the present

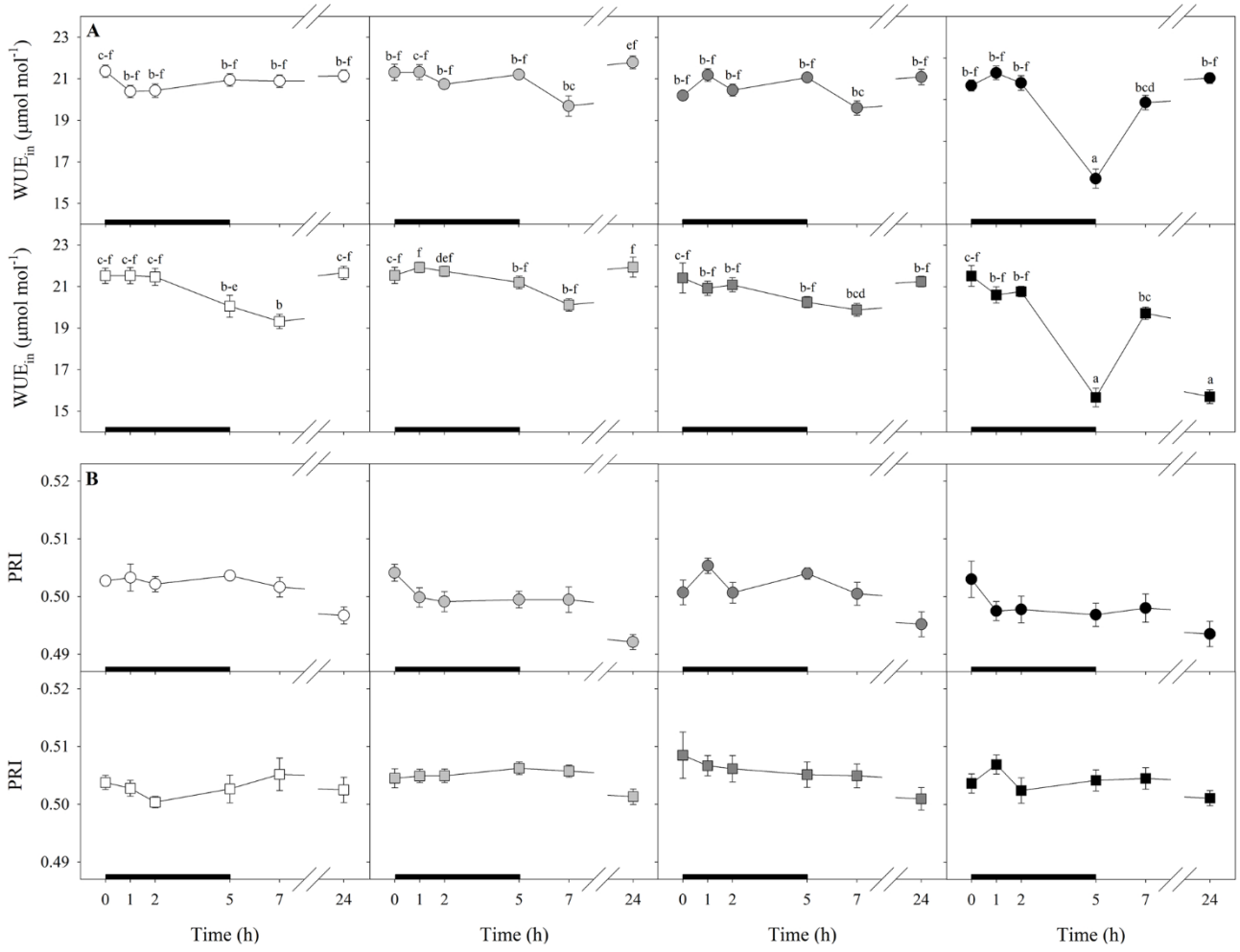

Fig. 4. Variation in intrinsic water use efficiency (WUE_{in}, A) and photochemical reflectance index (PRI, B) in pomegranate cultivars Parfianka (circle) and Wonderful (square) exposed to 0 (white), 50 (light gray), 100 (dark gray) or 200 ppb (black) of ozone (O_3) for 5 h. Measurements were carried out at 0, 1, 2, 5, 7 and 24 h from the beginning of exposure. Data are shown as mean ± standard error. Since three-way repeated measures ANOVA reveals a significant cultivar × O_3 × time interaction on WUE_{in} (see Table 3), according to Tukey's *post-hoc* test, different letters indicate significant differences among means ($P \leq 0.05$). The thick black bar indicates the time of O_3 exposure (i.e. 5 h).

study was the concomitant prediction from spectra of numerous widely used leaf traits related to oxidative pressure induced by O_3 on plants. We firstly focused on photosynthesis since it is a major plant process that is severely affected by O_3, usually by both stomatal and mesophyll constraints (Ainsworth, 2017). Standard collections of CO_2- and light-saturated photosynthesis, however, are sometimes logistically challenging, usually requiring several minutes per leaf. Spectral approaches have been shown as a valid alternative to these standard measurements since are able to estimate photosynthetic activity in plants. Vegetation indices correlated with photosynthetic processes are known (e.g. the xanthophyll cycle by PRI; Gamon et al., 1997; Peñuelas et al., 2011). Furthermore, specific and commonly used photosynthetic traits have been directly predicted from spectral data, using multivariate methods. However, few parameters have been investigated so far, mainly the maximum rate of carboxylation (V_{cmax}) and the maximum rate of electron transport (J_{max}; e.g. Serbin et al., 2012; Ainsworth et al., 2014; Heckmann et al., 2017; Yendrek et al., 2017; Fu et al., 2020), and never in pomegranate. Unexpectedly, among PLSR-modeled gas-exchange traits, we found a high prediction performance only for E and C_i (validation R^2: 0.60), and a moderate prediction accuracy for WUE_{in} (validation R^2: 0.50); whereas lower accuracies were observed for g_s and A (validation R^2: 0.48 and 0.37, respectively). Although a low performance in A prediction from spectra has been already reported using a similar PLSR approach (e.g. Heckmann et al., 2017), these outcomes are not in accordance with our previous results on sage (Marchica et al., 2019) and maize (Cotrozzi et al., 2020b). This might be due to some inaccuracies occurred with both spectral and standard gas-exchange measurements of pomegranate leaves, being these short-stemmed, oblong-lanceolate, small in size (*ca.* 5 cm long and 1 cm wide), with a meaningful midvein, and leathery. Conversely, it is not surprising that best predictions of gas-exchange traits were obtained using only the wavelengths from 400 to 900 nm. The use of narrower ranges including only specific absorption wavelengths for the trait to estimate sometimes leads to better predictions than using the full range, since the incorporation of other spectral regions may reduce the prediction ability of those trait-specific wavelengths (Cotrozzi et al., 2018b; Marchica et al., 2019). Indeed, the 400−900 nm spectral range finally used for estimations of gas-exchange traits includes leaf pigment absorption features (Merzlyak et al., 2003), as well as the red-edge (700−750 nm; Mutanga and Skidmore, 2007). The importance of this pigment-related spectral region in the assessment of the photosynthetic processes has been largely shown (e.g. Gamon et al., 1997; Merzlyak et al., 2003; Serbin et al., 2012; Yendrek et al., 2017). Several studies have also reported that the shape of the red-edge is dependent on chlorophyll content (e.g. Smith et al., 2004; Zarco-Tejada et al., 2004) and stress conditions (e.g. Mutanga and Skidmore, 2007; Cotrozzi et al., 2018b). This supports the importance of wavelengths from 650 to 750 nm in predicting gas-exchange traits highlighted by coefficient and VIP profiles of the

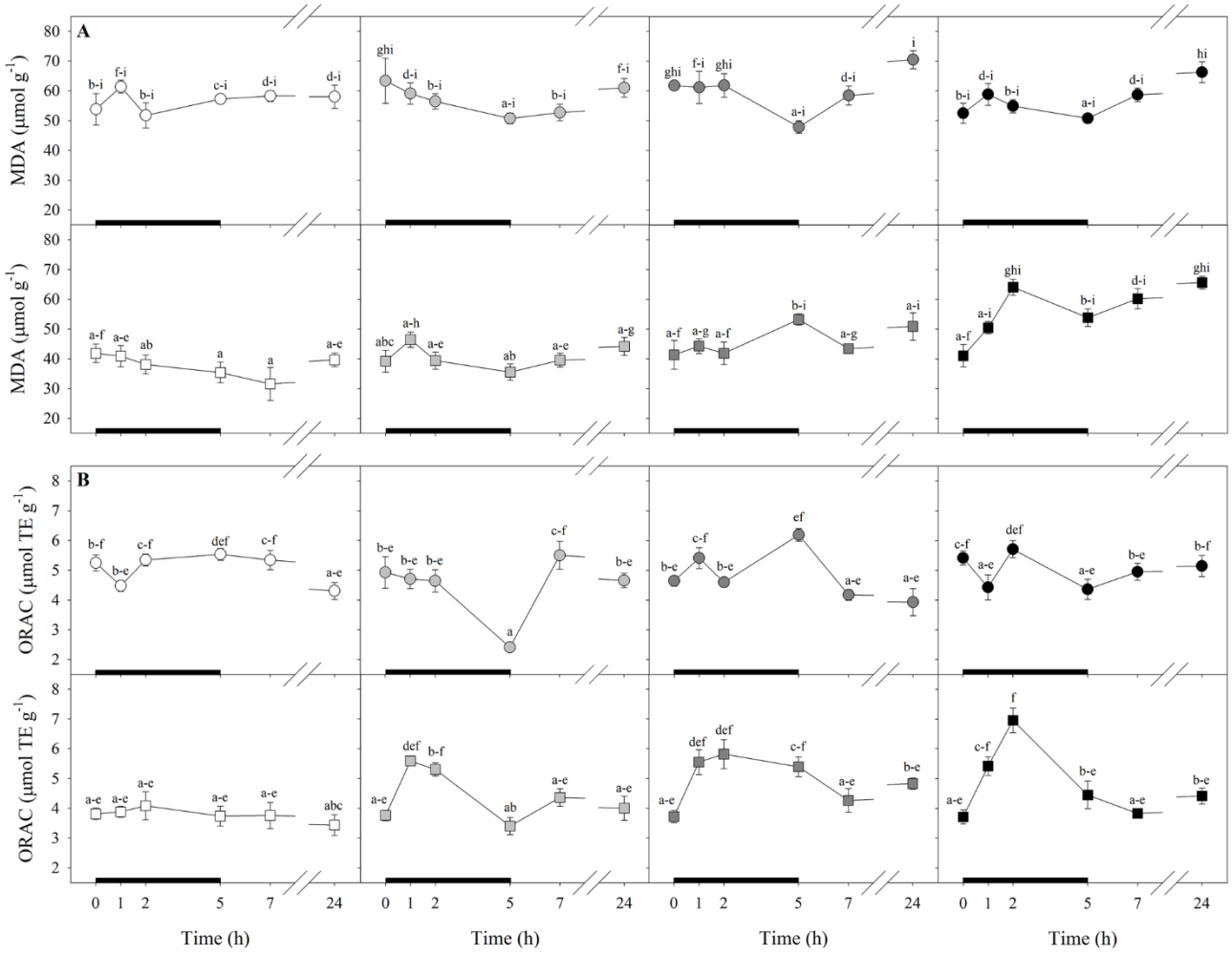

Fig. 5. Variation in malondialdehyde (MDA, A) and oxygen radical absorption capacity (ORAC, B) in pomegranate cultivars Parfianka (circle) and Wonderful (square) exposed to 0 (white), 50 (light gray), 100 (dark gray) or 200 ppb (black) of ozone (O_3) for 5 h. Measurements were carried out at 0, 1, 2, 5, 7 and 24 h from the beginning of exposure. Data are shown as mean ± standard error. Since three-way repeated measures ANOVA reveals a significant cultivar × O_3 × time interaction on both MDA and ORAC (see Table 3), according to Tukey's *post-hoc* test, different letters indicate significant differences among means ($P \leq 0.05$). The thick black bar indicates the time of O_3 exposure (i.e. 5 h). TE: trolox equivalents; GAE: gallic acid equivalents. Results are expressed on a dry weight basis.

PLSR-models here developed.

Although stomatal closure is the first response that leaves adopt against O_3 in order to limit its uptake, plants have also developed enzymatic (e.g. superoxide dismutase, catalase, and ascorbate peroxidase) and non-enzymatic (e.g. carotenoids, Asc, Glut, Phen and Ant) antioxidant systems to cope with the oxidative pressure due to the extensive amount of reactive oxygen species (ROS) generated by the rapid degradation of O_3 in the leaf cell apoplast (Gill and Tuteja, 2010; Pellegrini et al., 2016; Pistelli et al., 2019; Podda et al., 2019). The assessment of these traits by standard biochemical analyses may be precise, but has several limitations since these methods are destructive, time consuming and expensive, all aspects that make these investigations logistically challenging for monitoring a large number of individual plants. Here, we developed PLSR-models to predict from spectral data a number of widely used leaf traits related to the lipid peroxidation (MDA) induced by O_3, as well as the antioxidant capacity (ORAC and HORAC), and the main enzymatic (SOD_{act}, CAT_{act} and APX_{act}) and non-enzymatic antioxidants of plants (Asc, Glut, Phen and Ant). We had already developed PLSR-models for predicting some of these traits from sage spectra (Marchica et al., 2019). Yendrek et al. (2017) used the same approach to derive ORAC from maize reflectance data. However, spectral estimations of enzymatic antioxidants were never investigated before the present study. Interestingly, we found excellent prediction performance for Phen, ORAC and Ant (validation R^2: 0.77, 0.61 and 0.59, respectively), whereas moderate accuracy was observed for MDA and SOD_{act} (validation R^2: 0.56 and 0.50, respectively). Conversely, the models for HORAC, APX_{act}, and Asc showed lower performances (validation R^2: 0.44 for HORAC and APX_{cat}, and 0.45 for Asc), and even lower accuracies were found for Glut and CAT_{act}. The capability of spectroscopy data to accurately predict Phen is in accordance with previous studies (e.g. Campos-Medina et al., 2019; Cotrozzi and Couture, 2020), whereas the prediction outputs of models here developed for the other traits are lower than those we reported on sage (Marchica et al., 2019). These inconsistencies between the present study and previous investigations suggest that these outcomes are likely species- and stress condition-specific, as well as that improvement in modeling methods is needed, as previously reported (Marchica et al., 2019). Also for these traits, best predictions were reported using narrower ranges including only specific absorption features, except for APX_{cat} (400−2400 nm). Similarly to gas-exchange traits, MDA, ORAC, SOD_{act} and Glut were best predicted focusing on the pigment-related wavelengths and the red-edge (600−900, 400−800, 600−900 and 500−1100 nm, respectively), and the sensitivity of these foliar spectral features to oxidative stress induced by O_3 was further highlighted by coefficient and VIP profiles of these models. Conversely, HORAC, CAT_{act}, Asc and Phen best performed using longer NIR-SWIR regions

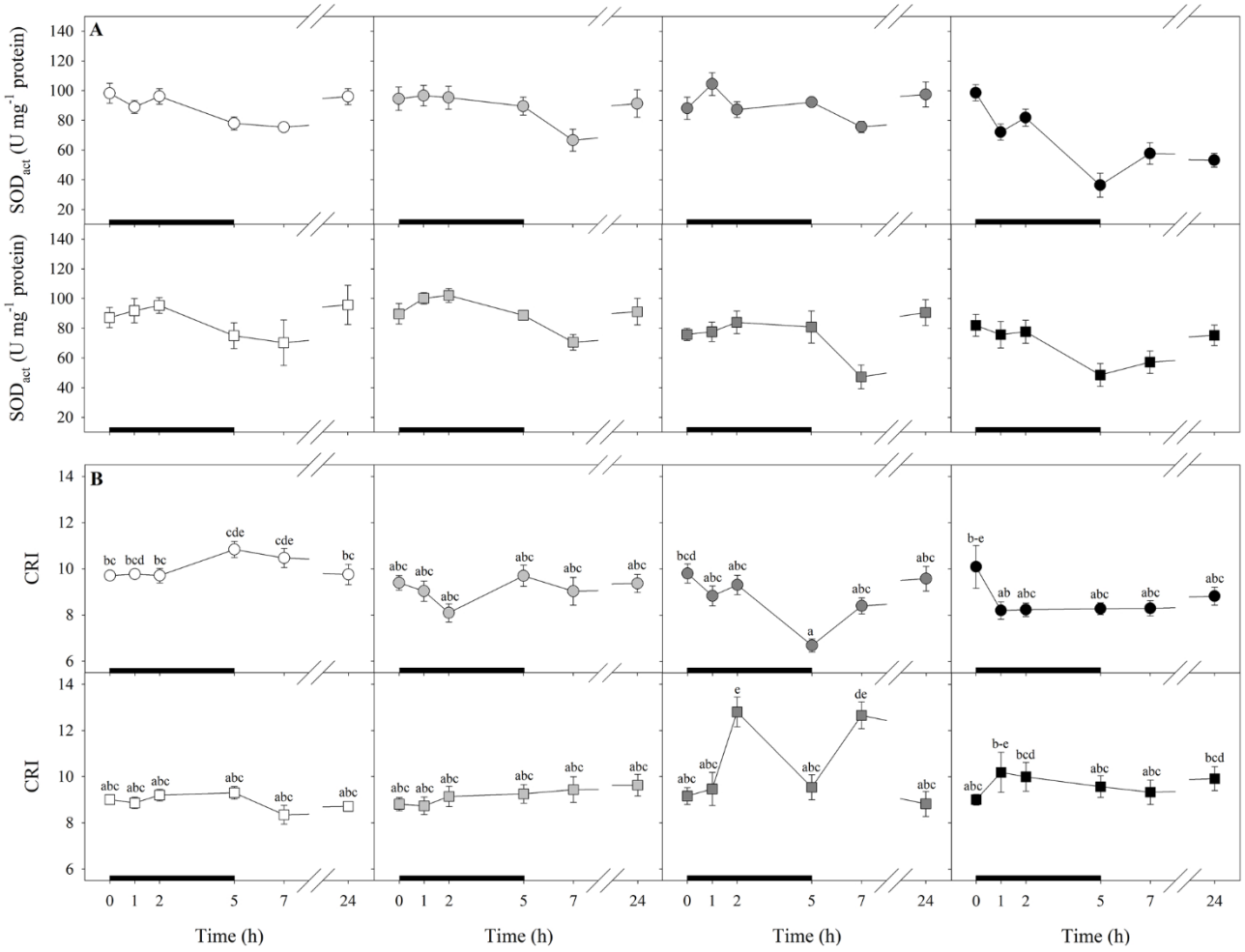

Fig. 6. Variation in superoxide dismutase activity (SOD_{act}, A) and carotenoid reflectance index (CRI, B) in pomegranate cultivars Parfianka (circle) and Wonderful (square) exposed to 0 (white), 50 (light gray), 100 (dark gray) or 200 ppb (black) of ozone (O_3) for 5 h. Measurements were carried out at 0, 1, 2, 5, 7 and 24 h from the beginning of exposure. Data are shown as mean ± standard error. Since three-way repeated measures ANOVA reveals a significant cultivar × O_3 × time interaction on CRI (see Table 3), according to Tukey's *post-hoc* test, different letters indicate significant differences among means ($P \leq 0.05$). The thick black bar indicates the time of O_3 exposure (i.e. 5 h).

(950−2400, 1400−2400, 1100−1800 and 1600−2400 nm, respectively), which are characterized by absorption features of larger molecules such as carbohydrates, proteins and water (Cotrozzi et al., 2018b). Indeed, coefficient and VIP profiles of these PLSR-models highlighted important wavelengths around 1400, 1700 and 1900 nm (also around 750 nm for APX_{cat}), according with previous reports about the remote sensing of foliar chemistry (Curran, 1989; Bolster et al., 1996; Serbin et al., 2014; Cotrozzi et al., 2018b). Although the approach proposed here may have limitations in discriminating fine scale variations of some biochemical traits (and we thus suggest caution when deciphering results from a small range of values), the present study also shows the potential to expand prediction capabilities of reflectance data for important and commonly investigated leaf biochemical features involved in the response of plants to oxidative pressure.

An overall benefit of the present study is that it concretely shows the potential of using the abovementioned and complementary spectroscopic approaches for investigating plant/stress interactions. The analyses of spectral signatures suggested two main interpretations: (i) a good tolerance of pomegranate to O_3 episodes, since it seemed substantially affected only by the highest O_3 concentration (i.e. 200 ppb), although negative effects induced by a chronic O_3 exposure on pomegranate cultivar Dente di cavallo were reported (Calzone et al., 2019); and (ii) an higher O_3 tolerance of cultivar Parfianka than Wonderful. These responses were confirmed by variations of the investigated vegetation indices and leaf traits derived from spectra (again, only leaf traits estimated with most accurate PLSR-models were used). Normalized different vegetation index, sPSRI and E variations respectively indicated that the 200 ppb O_3 episode induced changes in leaf greenness (even if no visible symptoms were detected during measurements, this being another good example of spectroscopy potential), senescing processes, and impairments to the photosynthetic activity. The occurrence of negative effects on the photosynthetic performance was confirmed by reductions of WUE_{in} observed in all plants at 5 h, and again only in Wonderful at 24 h, confirming the higher O_3 sensitivity of this cultivar. Actually, no other O_3-induced adverse effects were observed on Parfianka, except for a slight reduction of sPRI likely due to a reorganization of the xanthophyll cycle (Peñuelas et al., 2011). The WUE_{in} reductions, together with unchanged C_i values, suggested that both stomatal and mesophyll limitations occurred. Effectively, increased lipid peroxidation was observed only in Wonderful, from 2 h FBE to the end of the experiment. This was likely due to decreases in secondary metabolites, since Phen were similarly reduced by O_3 from 1 to 24 h FBE, and Ant dropped at the end of the exposure (i.e. 5 h FBE), likely when highest oxidative pressure occurred, as confirmed by variations of spectral signatures. The role of secondary metabolites in plant defense against abiotic stress is largely known (Ashraf et al., 2018; Naikoo et al., 2019). This outcome was supported by the inability of Wonderful plants to activate a proper antioxidant response since ORAC increased only at 2 h FBE, SOD_{act}

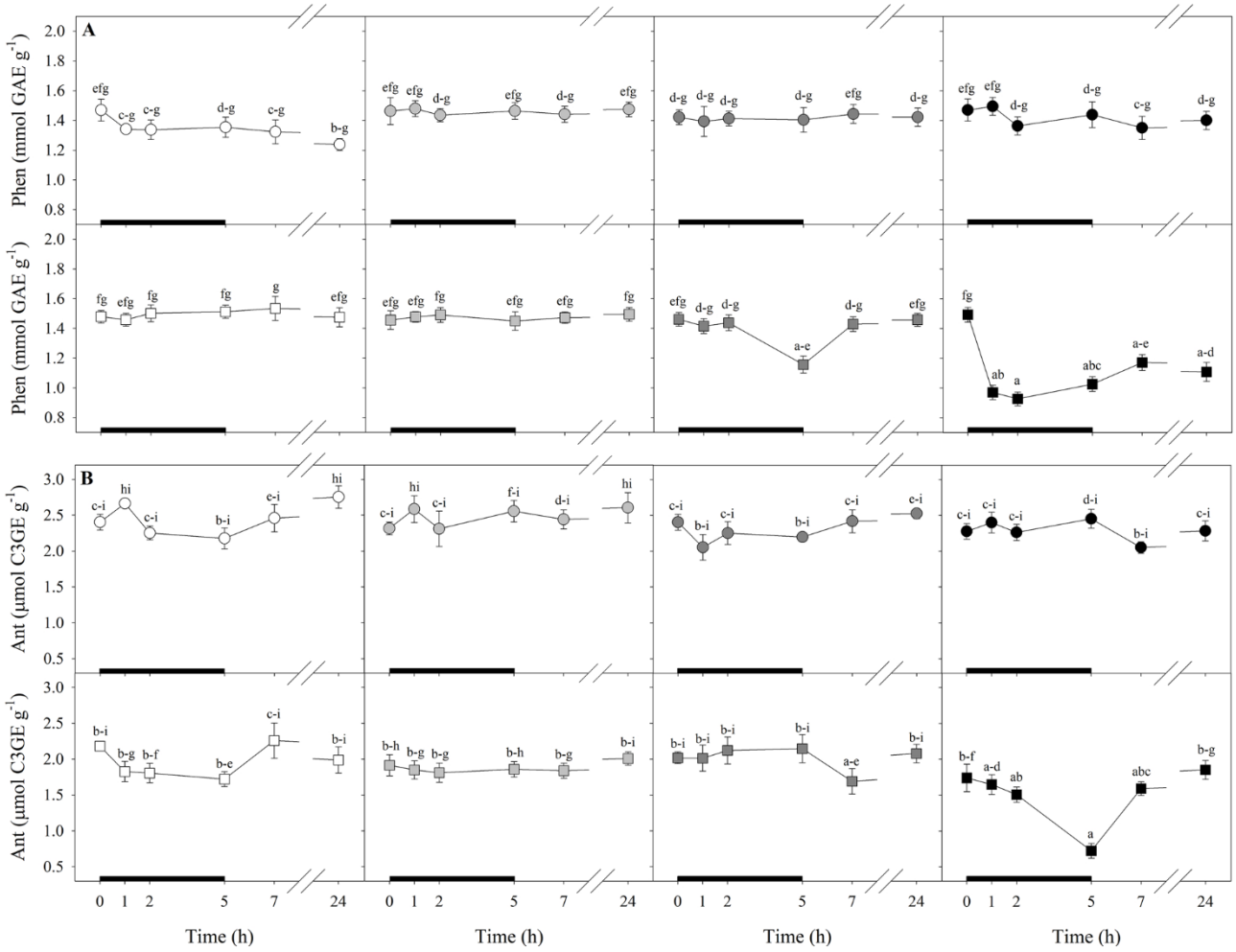

Fig. 7. Variation in total phenols (Phen, A) and anthocyanins (Ant, B) in pomegranate cultivars Parfianka (circle) and Wonderful (square) exposed to 0 (white), 50 (light gray), 100 (dark gray) or 200 ppb (black) of ozone (O_3) for 5 h. Measurements were carried out at 0, 1, 2, 5, 7 and 24 h from the beginning of exposure. Data are shown as mean ± standard error. Since three-way repeated measures ANOVA reveals a significant cultivar × O_3 × time interaction on both Phen and Ant (see Table 3), according to Tukey's *post-hoc* test, different letters indicate significant differences among means ($P \leq 0.05$). The thick black bar indicates the time of O_3 exposure (i.e. 5 h). GAE: gallic acid equivalents; C3GE: cyanidin 3-glucoside equivalents Results are expressed on a dry weight basis.

decreased (in both cultivars, actually), and an accumulation of carotenoids (CRI) did not occur. An increase of CRI was instead observed in Wonderful under 100 ppb, at 2 and 7 h FBE, likely to cope with harmful conditions observed at 5 h FBE, as demonstrated by the increase of MDA occurred at this time, as well as by changes in spectral signatures. Also in this case, the enhanced lipid peroxidation was twinned with a reduction of Phen, confirming the role of these compounds in plant defense (e.g. consumption of these compounds by the cell to counteract the accumulation of H_2O_2). These variations confirm the higher O_3 sensitivity of Wonderful than Parfianka, since Parfianka, in accordance to the analyses of spectral signatures, did not show any leaf trait changes under 100 ppb (CRI decreased at 5 h FBE, actually). The 50 ppb concentration was confirmed to not affect pomegranate (further investigations would be needed to explain the ORAC decrease at 5 h FBE, since no changes were observed among the investigated antioxidants). Overall, the responses shown by our cultivars to cope with O_3 episodes are in accordance with previous reports (e.g. Kangasjärvi et al., 2005; Vainonen and Kangasjärvi, 2015).

5. Conclusions

In conclusion, the present study confirms that spectral information can accurately identify different cultivars of the same species, as well as oxidative stress conditions in plants exposed to a gradient of O_3 concentration episodes. This spectral detection works also in the absence of visible symptoms and using O_3-tolerant plants/cultivars like pomegranate (especially the cultivar Parfianka). Furthermore, this study confirms that vegetation spectroscopy can be a rapid, non-destructive, and relatively inexpensive tool to concomitantly and accurately estimate an array of widely used physiological and biochemical leaf traits (some of them never investigated before) associated with oxidative stress/plant interaction, using a single spectral measurement. The present study also shows limitations of the proposed approach, such as in discriminating interactive effects from spectral profiles, especially for tolerant cultivars, and under mild stress conditions. In the same way, limits are evident in predicting specific leaf traits from spectra collected on leaves that are morphologically challenging to measure. Nevertheless, outcomes and approaches presented in the current study could be of application in a number of scientific fields such as precision agriculture and high-throughput plant phenotyping, and could provide significant benefits to achieve greater plant yield and quality (and incomes), with lower environmental impact.

CRediT authorship contribution statement

Antonella Calzone: Investigation, Formal analysis, Writing - original draft. **Lorenzo Cotrozzi:** Conceptualization, Methodology, Formal analysis, Data curation, Writing - original draft. **Damiano Remorini:**

Methodology, Writing - review & editing. **Giacomo Lorenzini:** Conceptualization, Writing - review & editing, Resources. **Cristina Nali:** Conceptualization, Resources. **Elisa Pellegrini:** Conceptualization, Writing - review & editing, Resources, Supervision.

Declaration of Competing Interest

The authors declare no conflict of interest.

Acknowledgments

Authors gratefully acknowledge Francesco Pitta for helping with spectral measurements and data organization, and Andrea Parrini for supervising the growth chamber and the ozone exposure facilities.

This research did not receive any specific grant from funding agencies in the public, commercial, or not-for-profit sectors.

Appendix A. Supplementary data

Supplementary material related to this article can be found, in the online version, at doi:https://doi.org/10.1016/j.envexpbot.2020.104309.

References

Aebi, H., 1984. Catalase in vitro. Methods Enzymolol. 105, 121–123. https://doi.org/10.1016/S0076-6879(84)05016-3.

Ainsworth, E.A., 2017. Understanding and improving global crop response to ozone pollution. Plant J. 90, 886–897. https://doi.org/10.1111/tpj.13298.

Ainsworth, E.A., Gillespie, K.M., 2007. Estimation of total phenolic content and other oxidation substrates in plant tissues using Folin-Ciocalteau reagent. Nat. Protoc. 4, 875–877. https://doi.org/10.1038/nprot.2007.102.

Ainsworth, E.A., Serbin, S.P., Skoneczka, J.A., Townsend, P.A., 2014. Using leaf optical properties to detect ozone effects on foliar biochemistry. Photosyn. Res. 119, 65–76. https://doi.org/10.1007/s11120-013-9837-y.

Anderson, M.J., 2001. A new method for non-parametric multivariate analysis of variance. Austral Ecol. 26, 32–46. https://doi.org/10.1111/j.1442-9993.2001.01070.pp.x.

Ashraf, M.A., Iqbal, M., Rasheed, R., Hussain, I., Riaz, M., Arif, M.S., 2018. Environmental stress and secondary metabolites in plants: an overview. In: Ahmad, P., Ahanger, M.A., Singh, V.P., Tripathi, D.K., Alam, P., Alyemeni, M.N. (Eds.), Plant Metabolites and Regulation Under Environmental Stress. Academic Press, London, pp. 153–167.

Atzberger, C., Guerif, M., Baret, F., Werner, W., 2010. Comparative analysis of three chemometric techniques for the spectrometric assessment of canopy chlorophyll content in winter wheat. Comput. Electron. Agric. 73, 165–173. https://doi.org/10.1111/10.1016/j.compag.2010.05.006.

Begum, H., Alam, M.S., Feng, Y., Koua, P., Ashrafuzzman, M., Shrestha, A., Kamruzzaman, M., Dadshani, S., Ballvora, A., Naz, A.A., Frei, M., 2020. Genetic dissecation of bread wheat diversity and identification of adaptive loci in response to elevated tropospheric ozone. Plant Cell Environ. 43, 2650–2665. https://doi.org/10.1111/pce.13864.

Bolster, K.L., Martin, M.E., Aber, J.D., 1996. Determination of carbon fraction and nitrogen concentration in tree foliage by near infrared reflectance: a comparison of statistical methods. Can. J. For. Res. 26, 590–600. https://doi.org/10.1139/x26-068.

Bradford, M., 1976. A rapid and sensitive method for the quantitation of microgram quantities of protein utilizing the principle of protein-dye binding. Anal. Biochem. 72, 248–254. https://doi.org/10.1006/abio.1976.9999.

Calzone, A., Podda, A., Lorenzini, G., Maserti, B.E., Carrari, E., Deleanu, E., Hoshika, Y., Haworth, M., Nali, C., Badea, O., Pellegrini, E., Fares, S., Paoletti, E., 2019. Cross-talk between physiological and biochemical adjustments by *Punica granatum* cv. Dente di cavallo mitigates the effects of salinity and ozone stress. Sci. Total Environ. 656, 589–597. https://doi.org/10.1016/j.scitotenv.2018.11.402.

Calzone, A., Cotrozzi, L., Pellegrini, E., Guidi, L., Lorenzini, G., Nali, C., 2020. Differential response strategies of pomegranate cultivars lead to similar tolerance to increasing salt concentrations. Sci. Hortic. 271, 109441. https://doi.org/10.1016/j.scienta.2020.109441.

Campos-Medina, V.A., Cotrozzi, L., Stuart, J.J., Couture, J.J., 2019. Spectral characterization of wheat functional trait responses to Hessian fly: mechanisms for trait-based resistance. PLoS One 14, e0219431. https://doi.org/10.1371/journal.pone.0219431.

Catola, S., Marino, G., Emiliani, G., Huseynova, T., Musayev, M., Akparov, Z., Maserti, B. E., 2016. Physiological and metabolomic analysis of *Punica granatum* (L.) under drought stress. Planta 243, 441–449. https://doi.org/10.1371/10.1007/s00425-015-2414-1.

Cavender-Bares, J., Meireles, J.E., Couture, J.J., Kaproth, M.A., Kingdon, C.C., Singh, A., Serbin, S.P., Center, A., Zuniga, E., Pilz, G., Townsend, P.A., 2016. Associations of leaf spectra with genetic and phylogenetic variation in oaks: prospects for remote detection of biodiversity. Remote Sens. 8, 221. https://doi.org/10.3390/rs8030221.

Cevallos-Casals, B.A., Cisneros-Zevallos, L., 2003. Stoichiometric and kinetic studies of phenolic antioxidants from Andean purple corn and red-fleshed sweet potato. J. Agric. Food Chem. 51, 3313–3319. https://doi.org/10.1021/jf034109c.

Chen, S., Hong, X., Harris, C.J., Sharkey, P.M., 2004. Sparse modeling using orthogonal forest regression with PRESS statistic and regularization. IEEE Trans. Syst. Man Cybernetics Part B (Cybernetics) 34, 898–911. https://doi.org/10.1109/tsmcb.2003.817107.

Chevallier, S., Bertand, D., Kohler, A., Courcoux, P., 2006. Application of PLS-DA in multivariate image analysis. J. Chemom. 20, 221–229. https://doi.org/10.1002/cem.994.

Chong, I.-G., Jun, C.-H., 2005. Performance of some variable selection methods when multicollinearity is present. Chemom. Intell. Lab. Syst. 28, 103–112. https://doi.org/10.1016/j.chemolab.2004.12.011.

Cotrozzi, L., Couture, J.J., 2020. Hyperspectral assessment of plant responses to multi-stress environments: prospects for managing protected agrosystems. Plants People Planet 2, 244–258. https://doi.org/10.1002/ppp3.10080.

Cotrozzi, L., Couture, J.J., Cavender-Bares, J., Kingdon, C.C., Fallon, B., Pilz, G., Pellegrini, E., Nali, C., Townsend, P.A., 2017. Using foliar spectral properties to assess the effects of drought on plant water potential. Tree Physiol. 37, 1582–1591. https://doi.org/10.1093/treephys/tpx106.

Cotrozzi, L., Remorini, D., Pellegrini, E., Guidi, L., Nali, C., Lorenzini, G., Massai, R., Landi, M., 2018a. Living in a Mediterranean city in 2050: broadleaf or evergreen 'citizens'? Environ. Sci. Pollut. Res. - Int. 25, 8161–8173. https://doi.org/10.1007/s11356-017-9316-7.

Cotrozzi, L., Townsend, P.A., Pellegrini, E., Nali, C., Couture, J.J., 2018b. Reflectance spectroscopy: a novel approach to better understand and monitor the impact of air pollution on Mediterranean plants. Environ. Sci. Pollut. Res. - Int. 25, 8249–8267. https://doi.org/10.1007/s11356-017-9568-2.

Cotrozzi, L., Lorenzini, G., Nali, C., Pellegrini, E., Saponaro, V., Hoshika, Y., Arab, L., Rennenberg, H., Paoletti, E., 2020a. Hyperspectral reflectance of light-adapted leaves can predict both dark- and light-adapted Chl fluorescence parameters, and the effects of chronic ozone exposure on date palm (*Phoenix dactylifera*). Int. J. Mol. Sci. 21, 6441. https://doi.org/10.3390/ijms21176441Cotrozzi.

Cotrozzi, L., Peron, R., Tuinstra, M.R., Mickelbart, M.V., Couture, J.J., 2020b. Spectral phenotyping of physiological and anatomical leaf traits related with maize water status. Plant Physiol. 184, 1363–1377. https://doi.org/10.1104/pp.20.00577.

Couture, J.J., Singh, A., Rubert-Nason, K.F., Serbin, S.P., Lindroth, R.L., Townsend, P.A., 2016. Spectroscopic determination of ecologically relevant plant secondary metabolites. Methods Ecol. Evol. 7, 1402–1412. https://doi.org/10.1111/2041-210X.12596.

Curran, P.J., 1989. Remote sensing of foliar chemistry. Remote Sens. Environ. 30, 271–278. https://doi.org/10.1016/0034-4257(89)90069-2.

Dixon, P., 2003. VEGAN, a package of R functions for community ecology. J. Veg. Sci. 14, 927–930. https://doi.org/10.1111/j.1654-1103.2003.tb02228.x.

Ely, K.S., Burnett, A.C., Lieberman-Cribbin, W., Serbin, S.P., Rogers, A., 2019. Spectroscopy can predict key leaf traits associated with source-sink balance and carbon-nitrogen status. J. Exp. Bot. 70, 1789–1799. https://doi.org/10.1093/jxb/erz061.

Fu, P., Meacham-Hensold, K., Guan, K., Wu, J., Bernacchi, C., 2020. Estimating photosynthetic traits from reflectance spectra: A synthesis of spectral indices, numerical inversion, and partial least square regression. Plant Cell Environ. 43, 1241–1258. https://doi.org/10.1111/pce.13718.

Gamon, J.A., Field, C.B., Goulden, M.L., Griffin, K.L., Hartley, A.E., Joel, G., Peñuelas, J., Valentini, R., 1995. Relationships between NDVI, canopy structure, and photosynthesis in three Californian vegetation types. Ecol. Appl. 5, 28–41. https://doi.org/10.2307/1942049.

Gamon, J.A., Serrano, L., Surfus, J.S., 1997. The photochemical reflectance index: an optical indicator of photosynthetic radiation use efficiency across species, functional types, and nutrient levels. Oecologia 112, 492–501. https://doi.org/10.1007/s004420050337.

Gill, S.S., Tuteja, N., 2010. Reactive oxygen species and antioxidant machinery in abiotic stress tolerance in crop plants. Plant Physiol. Biochem. 48, 909–930. https://doi.org/10.1016/j.plaphy.2010.08.016.

Gitelson, A.A., Zur, Y., Chivkunova, O.B., Merzlyak, M.N., 2002. Assessing carotenoid content in plant leaves with reflectance spectroscopy. Photochem. Photobiol. 75, 272–281. https://doi.org/10.1562/0031-8655(2002)075<0272:accipl>2.0.co;2.

Gongora-Canul, C., Salgado, J.D., Singh, D., Cruz, A.P., Cotrozzi, L., Couture, J., Rivadeneira, M.G., Cruppe, G., Valent, B., Todd, T., Poland, J., Cruz, C.D., 2020. Temporal dynamics of wheat blast epidemics and disease measurements using multispectral imagery. Phytopathology 110, 393–405. https://doi.org/10.1094/PHYTO-08-19-0297-R.

Grossman, Y.L., Ustin, S.L., Jacquemond, S., Sanderson, E.W., Schmuck, G., Verdebout, J., 1996. Critique of stepwise multiple linear regression for the extraction of leaf biochemistry information from leaf reflectance data. Remote Sens. Environ. 56, 182–193. https://doi.org/10.1016/0034-4257(95)00235-9.

Guidi, L., Remorini, D., Cotrozzi, L., Giordani, T., Lorenzini, G., Massai, R., Nali, C., Natali, L., Pellegrini, E., Trivellini, A., Vangelisti, A., Vernieri, P., Landi, M., 2016. The harsh life of an urban tree: the effect of a single pulse of ozone in salt-stressed *Quercus ilex* saplings. Tree Physiol. 37, 246–260. https://doi.org/10.1093/treephys/tpw103.

Heckmann, D., Schlüter, U., Weber, A.P.M., 2017. Machine learning techniques for predicting crop photosynthetic capacity from leaf reflectance spectra. Mol. Plant 10, 878–890. https://doi.org/10.1016/j.molp.2017.04.009.

Hodges, D.M., DeLong, J.M., Forney, C.F., Prange, R.K., 1999. Improving the thiobarbituric acid reactive substances assay for estimating lipid peroxidation in plant tissues containing anthocyanin and other interfering compounds. Planta 207, 604–611. https://doi.org/10.1007/s004250050524.

Johanningsmeier, S.D., Harris, G.K., 2011. Pomegranate as a functional food and nutraceutical source. Annu. Rev. Food Sci. Technol. 2, 181–201. https://doi.org/10.1146/annurev-food-030810-153709.

Kampfenkel, K., Van Montagu, M., Inzé, D., 1995. Extraction and determination of ascorbate and dehydroascorbate from plant tissue. Anal. Biochem. 225, 165–167. https://doi.org/10.1006/abio.1995.1127.

Kangasjärvi, J., Jaspers, P., Kollist, H., 2005. Signalling and cell death in ozone-exposed plants. Plant Cell Environ. 28, 1021–1036. https://doi.org/10.1111/j.1365-3040.2005.01325.x.

Khodabakhshian, R., Emadi, B., Khojastehpour, M., Golzarian, M.R., 2019. A comparative study of reflectance and transmittance models of VIS/NIR spectroscopy used in determining internal quality attributes in pomegranate fruits. J. Food Meas. Charact. 13, 3130–3139. https://doi.org/10.1007/s11694-019-00235-z.

Kuhn, M., 2008. Building predictive models in R using the caret package. J. Stat. Softw. 28, 5. https://doi.org/10.18637/jss.v028.i05.

Landi, M., Cotrozzi, L., Pellegrini, E., Remorini, D., Tonelli, M., Trivellini, A., Nali, C., Guidi, L., Massai, R., Vernieri, P., Lorenzini, G., 2019. When "thirsty" means "less able to activate the signalling wave trigged by a pulse of ozone": a case of study in two Mediterranean deciduous oak species with different drought sensitivity. Sci. Total Environ. 657, 379–390. https://doi.org/10.1016/j.scitotenv.2018.12.012.

Lefohn, A.S., Malley, C.S., Smith, L., Wells, B., Hazucha, M., Simon, H., Naik, V., Mills, G., Schultz, M.G., Paoletti, E., De Marco, A., Xu, X., Zhang, L., Wang, T., Neufeld, H.S., Musselman, R.C., Tarasick, D., Brauer, M., Feng, Z., Tang, H., Kobayashi, K., Sicard, P., Solberg, S., Gerosa, G., 2018. Tropospheric ozone assessment report: global ozone metrics for climate change, human health, and crop/ecosystem research. Elementa Sci. Anthropocene 6, 28. https://doi.org/10.1525/elementa.279.

Marchica, A., Loré, S., Cotrozzi, L., Lorenzini, G., Nali, C., Pellegrini, E., Remorini, D., 2019. Early detection of sage (*Salvia officinalis* L.) responses to ozone using reflectance spectroscopy. Plants 8, 346. https://doi.org/10.3390/plants8090346.

Merzlyak, M.N., Gitelson, A.A., Chivkunova, O.B., Rakitin, V.Y., 1999. Non-destructive optical detection of pigment changes during leaf senescence and fruit ripening. Physiol. Plant. 106, 135–141. https://doi.org/10.1034/j.1399-3054.1999.106119.x.

Merzlyak, M.N., Gitelson, A.A., Chivkunova, O.B., Solovchenko, A.E., Pogosyan, S.I., 2003. Application of reflectance spectroscopy for analysis of higher plant pigments. Russ. J. Plant Physiol. 50, 704–710. https://doi.org/10.1023/A:1025608728405.

Mevik, B.H., Wehrens, R., Liland, K.H., 2016. Pls: Partial Least Squares and Principal Component Regression. R Package Version 2.6-0. https://CRAN.R-project.org/package=pls.

Mittler, B., Zilinskas, B.A., 1993. Detection of ascorbate peroxidase activity in native gels by inhibition of the ascorbate-dependent reduction of nitroblue tetrazolium. Anal. Biochem. 212, 540–546. https://doi.org/10.1006/abio.1993.1366.

Mutanga, O., Skidmore, A.K., 2007. Red edge shift and biochemical content in grass canopies. ISPRS J. Photogramm. Remote. Sens. 62, 34–42. https://doi.org/10.1016/j.isprsjprs.2007.02.001.

Naikoo, M.I., Dar, M.I., Raghib, F., Jaleel, H., Ahmad, B., Raina, A., Khan, F.A., Naushin, F., 2019. Role and regulation of plants phenolics in abiotic stress tolerance: an overview. In: Khan, M.I.R., Reddy, P.S., Ferrante, A., Khan, N.A. (Eds.), Plant Signaling Molecules. Woodhead Publishing, Sawston, pp. 157–168.

Ochoa-Hueso, R., Munzi, S., Alonso, R., Arróniz-Crespo, M., Avila, A., Bermejo, V., et al., 2017. Ecological impacts of atmospheric pollution and interactions with climate change in terrestrial ecosystems of the Mediterranean Basin: current research and future directions. Environ. Pollut. 227, 194–206. https://doi.org/10.1016/j.envpol.2017.04.062.

Ou, B., Hampsch-Woodill, M., Prior, R.L., 2001. Development and validation of an improved oxygen radical absorbance capacity assay using fluorescein as fluorescent probe. J. Agric. Food Chem. 49, 4619–4626. https://doi.org/10.1016/10.1021/jf010586o.

Ou, B., Hampsch-Woodill, M., Flanagan, J., Deemer, E.K., Prior, R.L., Huang, D., 2002. Novel fluorometric assay for hydroxyl radical prevention capacity using fluorescein as the probe. J. Agric. Food Chem. 50, 2772–2777. https://doi.org/10.1021/jf011480w.

Pellegrini, E., Trivellini, E., Cotrozzi, L., Vernieri, P., Nali, C., 2016. Involvement of phytohormones in plant responses to ozone. In: Ahammed, G., Yu, J.Q. (Eds.), Plant Hormones Under Challenging Environmental Factors. Springer, Dordrecht, pp. 215–245.

Pellegrini, E., Campanella, A., Cotrozzi, L., Tonelli, M., Nali, C., Lorenzini, G., 2018. Ozone primes changes in phytochemical parameters in the medicinal herb *Hypericum perforatum* (St. John's wort). Ind. Crops Prod. 126, 119–128. https://doi.org/10.1016/j.indcrop.2018.10.002.

Peñuelas, J., Garbulsky, M.F., Filella, I., 2011. Photochemical reflectance index (PRI) and remote sensing of plant CO_2 uptake. New Phytol. 191, 596–599. https://doi.org/10.1111/j.1469-8137.2011.03791.x.

Pistelli, L., Tonelli, M., Pellegrini, E., Cotrozzi, L., Pucciariello, C., Trivellini, A., Lorenzini, G., Nali, C., 2019. Accumulation of rosmarinic acid and behaviour of ROS processing systems in *Melissa officinalis* L. under heat stress. Ind. Crops Prod. 138, 111469 https://doi.org/10.1016/j.indcrop.2019.111469.

Podda, A., Pisuttu, C., Hoshika, Y., Pellegrini, E., Carrari, E., Lorenzini, G., Nali, C., Cotrozzi, L., Zhang, L., Baraldi, R., Neri, L., Paoletti, E., 2019. Can nutrient fertilization mitigate the effects of ozone exposure on an ozone-sensitive poplar clone? Sci. Total Environ. 657, 340–350. https://doi.org/10.1016/j.scitotenv.2018.11.459.

Serbin, S.P., Dillaway, D.N., Kruger, E.L., Townsend, P.A., 2012. Leaf optical properties reflect variation in photosynthetic metabolism and its sensitivity to temperature. J. Exp. Bot. 63, 489–502. https://doi.org/10.1093/jxb/err294.

Serbin, S.P., Singh, A., McNeil, B.E., Kingdon, C.C., Townsend, P.A., 2014. Spectroscopic determination of leaf morphological and biochemical traits for northern temperate and boreal tree species. Ecol. Appl. 24, 1651–1669. https://doi.org/10.1890/13-2110.1.

Serbin, S.P., Singh, A., Desai, A.R., Dubois, S.G., Jablosnki, A.D., Kingdon, C.C., Kruger, E.L., Townsend, P.A., 2015. Remotely estimating photosynthetic capacity, and its response to temperature, in vegetation canopies using imaging spectroscopy. Remote Sens. Environ. 167, 78–87. https://doi.org/10.1016/j.rse.2015.05.024.

Sgherri, C.L.M., Navari-Izzo, F., 1995. Sunflower seedlings subjected to increasing water deficit stress: oxidative stress and defence mechanisms. Physiol. Plant. 93, 25–30. https://doi.org/10.1034/j.1399-3054.1995.930105.x.

Singh, B., Singh, J.P., Kaur, A., Singh, N., 2018. Phenolic compounds as beneficial phytochemicals in pomegranate (*Punica granatum* L.) peel: a review. Food Chem. 261, 75–86. https://doi.org/10.1016/j.foodchem.2018.04.039.

Smith, K.L., Steven, M.D., Colls, J.J., 2004. Use of hyperspectral derivative tools in red-edge region to identify plant stress response to gas leaks. Remote Sens. Environ. 92, 207–212. https://doi.org/10.1016/j.rse.2004.06.002.

Texeira da Silva, J.A., Rana, T.S., Narzary, D., Verma, N., Meshram, D.T., Ranade, S.A., 2013. Pomegranate biology and biotechnology: a review. Sci. Hortic. 160, 85–107. https://doi.org/10.1016/j.scienta.2013.05.017.

Vainonen, J.P., Kangasjärvi, J., 2015. Plant signalling in acute ozone exposure. Plant Cell Environ. 38, 240–252. https://doi.org/10.1111/pce.12273.

Wold, S., Sjöström, M., Eriksson, L., 2001. PLS-regression: a basic tool of chemometrics. Chemom. Intell. Lab. Syst. 58, 109–130. https://doi.org/10.1016/S0169-7439(01)00155-1.

Yendrek, C.R., Tomaz, T., Montes, C.M., Cao, Y., Morse, A.M., Brown, P.J., McIntyre, L.M., Leakey, A.D.B., Ainsworth, E.A., 2017. High-throughput phenotyping maize leaf physiological and biochemical traits using hyperspectral reflectance. Plant Physiol. 173, 614–626. https://doi.org/10.1104/pp.16.01447.

Zarco-Tejada, P.J., Miller, J.R., Morales, A., Berjón, A., Agüera, J., 2004. Hyperspectral indices and model simulation for chlorophyll estimation in open-canopy tree crops. Remote Sens. Environ. 9, 463–476. https://doi.org/10.1016/j.rse.2004.01.017.

Zhang, J., Kirkham, M.B., 1994. Drought-stress-induced changes in activities of superoxide dismutase, catalase, and peroxidase in wheat species. Plant Cell Physiol. 35, 783–791. https://doi.org/10.1093/oxfordjournals.pcp.a078658.